치의과학박사학위논문

Effect of PAIP1 expression on metastatic potential and its prognostic significance in oral squamous cell carcinoma

PAIP1 발현이 구강 편평 세포 암종에서 전이능과 예후에 미치는 영향

2021 년 08 월

서울대학교 대학원

치의과학과 구강병리학전공

Neeti Swarup

Effect of PAIP1 expression on metastatic potential and its prognostic significance in oral squamous cell carcinoma

PAIP1 발현이 구강 편평 세포 암종에서 전이능과 예후에 미치는 영향

지도교수 홍 성 두

이 논문을 치의과학박사 학위논문으로 제출함

2021 년 06 월

서울대학교 대학원

치의과학과 구강병리학전공

Neeti Swarup

Neeti Swarup 의 박사 학위논문을 인준함

2021 년 07 월

위 원 장 _____

부 위 원 장 _____

위 원 _____

위 원 _____

위 원 _____

ABSTRACT

Effect of PAIP1 expression on metastatic potential and its prognostic significance in oral squamous cell carcinoma

Neeti Swarup

Department of Oral Pathology

Graduate School, Seoul National University

(Directed by Professor Seong-Doo Hong, D.D.S., M.S.D., Ph.D.)

Objectives: Lymph node metastasis (LNM) is a critical prognostic indicator for oral squamous cell carcinoma (OSCC). Biomarkers regulating LNM can serve as prognostic indicators and therapeutic targets. Dysregulation in translation machinery is a frequent feature in metastasis. PAIP1 (Poly Adenylate Binding Protein Interacting Protein 1) plays a critical role in translation initiation. The aim of the study was to understand the role of PAIP1 in regulating LNM in OSCC.

Methods: *In silico* and *in vitro* experiments along with immunohistochemistry on excised human tissues were employed to

conclude the role and mechanism by which PAIP1 affects LNM in OSCC. Data available on public domain from TCGA, CPTAC, GEO and CCLE databases was used to analyze PAIP1 expression in oral cancer. Additionally, PAIP1 silencing experiments were performed in oral cancer cell lines for determination of metastatic roles and mechanisms, using transwell collagen, matrigel assays, and gelatin zymography.

Results: Publicly available data suggests that PAIP1 was significantly upregulated in oral cancers at mRNA and protein levels when compared to normal tissues. Moreover, there was an increase in mRNA expression in cases of LNM. The IHC results suggest that PAIP1 was significantly upregulated in cancers when compared to normal oral epithelium, also stronger expressions were associated with increased tumor size, LNM and worse pattern of invasion. Following silencing of PAIP1 in oral cancer cell lines a significant reduction in colony forming abilities, migratory and invasive abilities were seen. Additionally, silencing of PAIP1 led to decrease in MMP-9 enzymatic activity, as seen on gelatin zymography. PAIP1 was found to affect the phosphorylation of c-SRC at tyrosine residue 419 and confirmed the correlation between PAIP1 and pSRC in human samples via IHC and CPTAC data analysis.

Conclusion: High PAIP1 expression was found to be associated with poor prognostic indicators of OSCC, like increased tumor size, LNM and advanced tumor stage. By means of *in vitro* and *in silico* experiments, it was seen that PAIP1 can regulate LNM in OSCC via activation of MMP-9 and affecting phosphorylation of c-SRC. Similarly the correlation between phosphorylation of c-SRC was seen to PAIP1 in excised human tissue samples. Taken together the results indicate that PAIP1 can be used as prognostic marker for OSCC, which can also be utilized as a therapeutic target.

Keywords: PAIP-1 protein, oral squamous cell carcinoma, invasion, Lymph Node Metastasis, Metastasis.

Student Number: 2018-37586

Table of Contents

I. Introduction

Oral cavity and pharyngeal cancers comprise of over 2% of all malignancies globally [1]. Squamous cell carcinoma is the most commonly occurring cancer of the mucosal linings of the oral cavity. Prognosis and management of oral cancer patients is dependent on the extent of primary tumor and distant metastasis [2]. Carcinogenesis is a multistep process, which can be broadly classified as: initiation, promotion, and progression [3]. Tumor metastasis is a critical step for tumor progression which depends on motility and invasion, plasticity of the cancer cells, modulation of the microenvironment, colonization by the cancer cells [4]. Lymph node metastasis (LNM) is one of the deterministic prognostic indicators in oral cancer [2] . Therefore, identifying biomarkers associated with LNM can aid in timely intervention and improved outcomes of Oral Squamous Cell Carcinoma (OSCC).

Translation machinery plays a critical role in regulation of gene expression to maintain cellular functions. Neoplasia is frequently characterized by dysfunction in translation regulatory mechanisms [5]. Translation efficiency depends on 5’ cap structure and 3’ poly (A) tail [6]. Translation initiation serves as the rate limiting step during translation [5]. Poly Adenylate binding protein (PABP) is said to be a critical translation initiation factor. PABP activity is chiefly regulated by Poly Adenylate

binding protein Interacting Protein 1 (PAIP1) and Poly Adenylate binding protein Interacting Protein 2 (PAIP2) [7].

PAIP1 was first identified by Sonenberg et al. in the year 1998 [8]. PAIP1 is located at 5p12, on the 5p arm which is frequently amplified in various cancers [9, 10]. PAIP1 is a 479 amino acids protein, which has three recognized isoforms. The molecular weights of different isoforms; p65, p51 and p45 of which p45 has the highest translation efficiency [11]. Role of PAIP1 is widely recognized during Cap dependent Translation Initiation, moreover it has also been described to be involved in Cap independent Translation Initiation via iRES dependent entry at the ribosomal unit [5]. It has a homology with eIF4G, which interacts with eIF4A and eIF3 complex to facilitate translation initiation. PAIP1 has PAM1 and PAM2 domains, domains, of which PAM1 interacts with the RRM 1 and 2 domains on PABP and PAM2 interacts with C-terminal domain of PABP [12]. Its interaction with eIF3 is regulated via S6 kinase [13]. PAIP1 therefore interacts with PABP, eIF4G, eIF3 to regulate translation initiation. These interactions help in circularization of RNA and aid in translation initiation [11]. Recently PAIP1 has been identified to interact with eRF3 and regulate translation termination as well, along with PAIP2 [14].

PAIP1 is frequently found upregulated in cancers and has been reported in various carcinomas including cervical and lung cancer. It has been identified to interact with various oncogenes to regulate different aspects of oncogenesis, like cellular proliferation, cell death, metastasis [15, 16]. c-

SRC is a protooncogene, which on activation has pleiotropic roles [17]. c-SRC activity is generally regulated by phosphorylation and dephosphorylation of tyrosine domains or interaction with binding proteins like PDGFR, FAK which bind to the SH-2 domain. The phosphorylation and dephosphorylation events are regulated by phosphatases enzymes and/or kinases. c-SRC activation is generally associated with phosphorylation of tyrosine 419 domain [18]. Activated SRC can trigger numerous downstream targets to regulates carcinogenesis.

The breach in the basement membrane and invasion of the stromal tissue, marks progression of metastasis [19]. Matrix metalloproteinases, also called as matrixins, can degrade different elements/ proteins in extra cellular matrix and/or stromal tissues. MMPs can be classified into various groups like; archetypal, gelatinases, matrilysins, furin activated MMPs. Gelatinases (MMP-2 and MMP-9) can degrade collagen, and gelatin and affect the invasion and migratory process in cancer cells [20].

The association between PAIP1 expression and oral cancer metastasis has not yet been described. The objective of the research was to analyze the expression pattern of PAIP1 in cases of OSCC and its association with different clinicopathologic and histopathologic features of OSCC. Identification of possible mechanistic target affected by PAIP1 was an additional objective.

II. Materials and Methods

In silico analysis

Secondary database analyses were done using online databases and software packages, as per data use agreements, for preliminary assessment of PAIP1 genomic alterations, mRNA expression, protein levels, and its relation to clinicopathologic parameters.

Gene Expression Omnibus (Geo Database)

Exploration for expression of PAIP1 mRNA was done using Geo database, https://www.ncbi.nlm.nih.gov/geo/. A differential expression analysis was done for GSE30784 [21] using Geo2R [22]. Variation in PAIP1 mRNA levels was investigated between the normal, dysplasia and cancer groups, using geo series GSE30784 reporter id 213754_s_at. The gcRMA normalized values were extracted for different GSM samples within the same study set using the series matrix file. Further, variation in PAIP1 mRNA levels was investigated within same cases between non tumor epithelia and tumor, using geo series GSE37991 [23] reporter id ILNM_1776398. The quantile normalized values were extracted for different GSM samples within the same study set using the series matrix file. The extracted data were converted to a log2 scale for plotting. Variation in PAIP1 mRNA levels were also investigated between the negative and positive nodal metastasis, using geo series GSE78060 reporter id

213754_s_at. The gcRMA normalized values were extracted for different GSM samples within the same study set using the series matrix file. The extracted data were converted to a log2 scale for plotting. All the extracted values were reconfirmed for normalization and analysis using Geo2R.

cBioportal

A pan cancer analysis was done for TCGA PanCan 2018 datasets for various tumors, using cBioportal, https://www.cbioportal.org/, to analyze genetic alterations associated with PAIP1 across epithelial origin tumors of different organs. Datasets for Clear Cell Renal Cell Carcinoma and Papillary Renal Cell Carcinoma were combined into single entry of Renal cancers and datasets for Glioblastoma Multiforme and Low-Grade Glioma were combined into single entry of Brain cancers. Tumors of mesenchymal origin and tumors with hybrid nature were not included for analysis and evaluation. Followed by analysis of genetic alterations, mRNA levels of PAIP1 were assessed for Head and Neck Cancer database in relation to log2 of copy-number values of PAIP1 [24].

UALCAN

A pan cancer analysis was done across TCGA Pan Cancer datasets for various tumors, using UALCAN, http://ualcan.path.uab.edu/index.html, to analyze variation in mRNA expression levels of PAIP1 across epithelial origin tumors of different organs. The distribution values were recorded and replotted [25].

Cancer Cell Line Encyclopedia (CCLE)

Following the assessment of clinical databases, cell line database, https://portals.broadinstitute.org/ccle was screened. A custom cohort was made from upper aerodigestive cell lines, including cell lines from tongue squamous cell carcinoma, squamous cell carcinoma of lower alveolus, oral cavity squamous cell carcinoma, gingival squamous cell carcinoma, head and neck basaloid carcinoma; to evaluate PAIP1 mRNA level in relation to PAIP1 copy number values.

The Cancer Genome Atlas (TCGA), Genomic Data Commons

A custom cohort was created from HNSC dataset, accessed via https://portal.gdc.cancer.gov/; including base of tongue, palate, lip, gum, tonsil, floor of mouth, other and unspecified parts of tongue, other and unspecified parts of mouth and; other and ill-defined sites in lip, oral cavity and pharynx. Expression levels of PAIP1 were analyzed using the FPKM-UQ files. The files were downloaded manually and data for PAIP1 was extracted using LINUX system. The data extracted were converted to log2 scale for analysis. The extraction, sorting and parsing code were custom developed using Jupyter notebook and Pandas on top of Python 3.0, the code can be found at (https://github.com/kunalchawlaa/TCGA-Oral-Cancer). The codes developed were based on suggestions provided on, https://labs.cd2h.org/gitforager/repository/repository.jsp?id=77901462. The results shown here are a part based upon data generated by the TCGA Research Network: https://www.cancer.gov/tcga.

Clinical Proteomic Tumor Analysis Consortium (CPTAC), Proteomic Data Commons

Proteomic levels for PAIP1 were evaluated and analyzed, for a custom cohort, accessed via https://pdc.cancer.gov/pdc/ including base of tongue NOS, tongue NOS, cheek mucosa, lip NOS, gum NOS, tonsil NOS, floor of mouth NOS, head, face or neck NOS and; overlapping lesion of lip, oral cavity and pharynx. Log values for Reporter ion intensity for unshared peptides of PAIP1 were extracted after downloading the file, CPTAC3_Head_and_Neck_Carcinoma_Proteome.tmt11.tsv and CPTAC3_Head_and_Neck_Carcinoma_Phosphoproteome.phosphopeptide.tmt11.tsv manually. The values obtained were used to compare expression level in normal and cancer [26].

Kaplan-Meier Plotter

Online available software, http://kmplot.com/analysis/index.php?p=background, was used to analyze and plot the association of PAIP1 levels to survival in HNSC patients. The software uses TCGA, GEO and EGA database for the mRNA values [27].

Clinical sample

Specimens were retrieved from 58 patients with OSCC who were surgically treated at the Department of Oral and Maxillofacial Surgery at Seoul National University Dental Hospital in the year 2009. Clinical data including age, sex, and recurrence were collected from patient medical

records. Classification of Tumors and staged according to the TNM system recommended by the American Joint Committee on Cancer [28]. Tumors were graded based on the World Health Organization (WHO) [29]. Histologic risk assessment was done to record the worst patterns of invasion (WPOI). WPOI 1, broad pushing tumor front; WPOI 2, finger-like pushing invasion; WPOI 3, large tumor islands > 15 cells; WPOI 4, small tumor island ≤ 15 cells or tumor strands; and WPOI 5, satellite tumor nodule at least 1 mm away from the main tumor [30]. The clinicopathological and histological features of the OSCC patients are summarized in Table 1 and 2. This study was approved by the Institutional Review Board (IRB) of Seoul National University Dental Hospital (IRB number: ERI20021).

Cell line selection

Eight oral cancer cell lines were screened along with a positive and negative control for PAIP1 protein and mRNA expression. HSC2, HSC3, HSC4, Ca9.22, HO1-N1 and HO1-U1 cells were kindly gifted by Hokkaido University (Hokkaido, Japan) and HN22 cells were kindly provided by Dankook University (Cheonan, Korea). SCC-9 cells and MDA-MB-231 were obtained from American Tissue Culture Collection (Manassas, VA, USA) and Korean Cell Line Bank (Seoul, Korea), respectively. iHOK cells were kindly provided by Yonsei University (Seoul, Korea). MDA-MB-231 was used as positive control and iHOK was used as negative control. Cells were seeded in DMEM-F12 or RPMI 1640 medium (Welgene, Daegu,

Korea), supplemented with 10% FBS and penicillin/streptomycin and KSF media (for iHOK cells) supplemented with BPE/EGFR at 37 °C, 5% CO_2 till they were 70-80% confluent.

Immunohistochemistry

Four μm serial sections were obtained from 58 OSCC and 36 adjacent normal oral mucosal tissue formalin-fixed, paraffin-embedded specimens. Specimens were serially sectioned for each case to detect PAIP1 and pSRC (Tyr419). One section per case was immunohistochemically stained using mouse monoclonal anti-PAIP1 (1:300 Santa Cruz, SC-365687) after heat induced antigen retrieval was performed in a microwave oven for 10 minutes in citrate buffer (pH 6.0) incubated overnight at 4 °C, followed by detection using Dako real detect HRP conjugated system. The other section was immunohistochemically stained after heat induced antigen retrieval was performed in a microwave oven for 8 minutes in citrate buffer (pH 6.0) using anti pSRC (Tyr419) (1:250, Invitrogen # 44-660G) incubated for 1 h at room temperature, followed by detection using Dako real detect HRP conjugated system. Slides incubated without primary antibody were used as a negative control.

Immunohistochemical Evaluation

Immunohistochemical staining was assessed semi-quantitatively by two oral pathologists, individually following blinding, in case of disagreement the

scores were reached to a consensus following discussion. Tumor cells showing cytoplasmic staining were considered positive. The tumor was differentiated into two zones: inner tumor mass and the invasive tumor front (most advanced layers and detached tumor cells). Both zones were scored independently [31] along with total tumor score. The percentage of positive cells was scored as follows: 0, <5%; 1, 5-25%; 2, 26–50%; and 3, 51–100%. Staining intensity was scored as follows: 0, negative; 1, weak (light brown); 2, moderate (brown); and 3, strong (dark brown). Each intensity score was added to the percentage score to generate a combined score. The final IHC score varies between 0-6. IHC scores between 0-2 were classified as negative; < 4 scores were classified as low while scores >4were classified as high. For statistical evaluation, the PAIP1 expression was dichotomized between low expression groups (comprising negative and low cases) and high expression groups (comprising high cases).

Immunoblot Analysis

Cells were collected following trypsinization. Cells were collected in RIPA buffer (Thermo Fisher Scientific) with protease inhibitor cocktail (Thermo Fisher Scientific), and then centrifuged at 15,000 × *g* at 4 °C for 15 min, followed by collection of the supernatant. Protein concentration was quantified using the DC Protein Assay Kit (BIO-RAD Laboratories, Madison, WI, USA). Protein samples were subsequently diluted with sample buffer, heated at 95 °C for 10 min. These samples were separated on

a 10–12% w/v SDS PAGE gel (Bio-Rad), and transferred to a polyvinylidene fluoride membrane. This membrane was blocked for 1 h in blocking solution, TBST (10 mM Tris, pH 8.0 and 0.1% v/v Tween 20), supplemented with 5% Difco Skim Milk (BD biosciences) and incubated in 1:1000 diluted solution of PAIP1 specific antibody (Santa Cruz, SC-365687), 1:1000 diluted solution of anti-GAPDH antibody (Abcam, ab9484), 1:1000 and 1:5000 diluted solution of anti-α-Tubulin (Santa Cruz, sc-5286), 1:1000 diluted solution of anti-SRC (Cell Signaling Technology, 2109s), 1:1000 diluted solution of anti-pSRC (Tyr416) (Cell Signaling Technology, 6943s), 1:1000 diluted solution of anti-MMP-9 (Cell Signaling Technology,3852s), 1:1000 diluted solution of E-Cadherin (sc-7870), 1:1000 diluted solution of N-Cadherin (610920), 1:2000 diluted solution of Zeb1 (NBP105987), 1:1000 diluted solution of Vimentin (sc-6260), 1:1000 diluted solution of Slug (c19G7), 1:1000 diluted solution of Snai1 (sc-271977), 1:1000 diluted solution of Twist (sc-81417) in TBST at 4 °C overnight. After washing (three washes for 5 min, 10 min, 15 min respectively) in TBST, membranes were treated accordingly for HRP-conjugated secondary antibodies, anti-mouse, or anti-rabbit. Finally, after washing with TBST, chemiluminescence was detected using SuperSignal WestPico Chemiluminescent Substrate (Santa Cruz Biotechnology Inc.) and were captured by Image Quant LAS 500 (GE Healthcare Life Sciences, Piscataway, NJ, USA).

Quantitative RT-PCR.

Total RNA was extracted using Trizol Reagent (Life Technologies, Carlsbad, CA, USA). One microgram of RNA was reverse-transcribed by an AMPIGENE cDNA Synthesis Kit (Enzo Life Sciences, Inc., NY, USA), and the resultant cDNA was subjected to PCR using AMPIGENE qPCR Green Mix Hi-Rox (Enzo Life Sciences, Inc.). Real-time PCR was performed using the Applied Biosystems StepOnePlus Real-Time PCR System (Applied Biosystems, Foster city, CA, USA) and PCR conditions for all genes were as follows: 95°C for 2 min, followed by 40 cycles of 95°C for 10 sec and 60°C for 30 s. The relative amount of each gene was normalized to the amount of GAPDH and calculated using the $2^{-\Delta\Delta CT}$ method [32]. The qPCR primers were: PAIP1 forward, 5′- TTT GGA AGA TGC TTG GAA GG -3′ PAIP1 reverse, 5′- TGA AGT TGC ATG GAC TCT GC -3′ (primer was designed using http://bioinfo.ut.ee/primer3-0.4.0/, by Cosmo genetech); GAPDH forward, 5′-GTGGTCTCCTCTGACTTCAAC-3′ GAPDH reverse, 5′-CCTGTTGCTGTAGCCAAATTC-3′.

Small-interfering (siRNA) RNA transfection.

siRNA transfection was performed with Bioneer predesigned siRNA reagent system (Bioneer, 10605-1) (sense 5′-CCAGGUGGUUGUAGCUCCU-3′, antisense 5′-AGGAGCUACAACCACCUGG-3′). siRNA was mixed with equal amount of DEPC to yield a concentration of 50 μM/ml. Cells were

seeded in 60 mm dish to 40-50% confluence in antibiotic-free 10% FBS-containing medium. For each transfection, 1 µl of PAIP1 siRNA, and unconjugated control siRNA in 49 µl of serum free DMEM-F12 were mixed with 5 µl of lipofectamine 2000 (sc-29528) in another 45 µl of transfection medium. The mixtures were incubated for 20 min at room temperature, to yield 25 nM concentration. Additionally, 2 µl of PAIP1 siRNA (Bioneer, 10605-1), and unconjugated control siRNA in 48 µl of serum free DMEM-F12 were mixed with 5 µl of lipofectamine 2000 (sc-29528) in another 45 µl of transfection medium. The mixtures were incubated for 20 min at room temperature, to yield 50 nM concentration. Each plate was washed twice with PBS and then filled with 1.9 ml of serum free DMEM-F12 followed by addition of 100 µl prepared reagent mixture. After 6 h incubation, the transfection media was removed and replaced with complete media containing 10% FBS and PS. The interference efficiency was checked following 24 h and 48 h. Two concentrations of 25 nM and 50 nM were used to test interference efficiency of the three PAIP1 mRNA variants. Interference experiments were performed using 10605-1, NM_006451.4, sense 5′-CCAGGUGGUUGUAGCUCCU-3′, antisense 5′-AGGAGCUACAACCACCUGG-3′ for 24 h with 25 nM concentration.

Proliferation Assay

The effect of PAIP1 interference on cell viability was investigated using the Trypan blue exclusion assay. Cells were harvested 24 h after RNA interference, stained with 0.4% trypan blue solution (Gibco; Thermo Fisher Scientific, Inc), and viable cells were counted using a hemocytometer.

Clonogenic Assay

siRNA treated cells were suspended in DMEM media supplemented with 10 % FBS and antibiotics were seeded in 6-well tissue culture plate (2000 cells/well) and were incubated at 37 °C, 5 % CO_2 in humidified air for 6–8 days depending on the growth. The media was changed every alternate day or as needed, and colonies (clusters of 20 or more cells) were scored under an inverted microscope after termination of the culture.

Transwell Migration Assay

The migration assay was performed using the Boyden chamber system (BD Falcon 8-μm pore, BD353097 with SPL 30024 cell culture plate, 24 well plate, SPL Life Sciences Co. Ltd., Gyeonggi-do, Korea). For the assay Collagen Type I, Rat Tail (BD 354236) was mixed with cold PBS to yield a concentration of 0.5 mg/ml. The basolateral side of the membrane on the transwell was coated with 10 μl collagen and PBS mixture. The transwell was incubated for 4 h at room temperature following coating with the

mixture. Cells following siRNA treatment were collected, and approximately 8×10^4 cells in 500 µl of serum free DMEM-F12 were placed into the upper boyden chamber. After adding 700 µl of DMEM-F12 with 10% FBS with P/S to the lower chamber, the assay plates were incubated at 37 °C in 5% CO_2 for 24 h. To assess the basal migration, cells that migrated to the underside of the upper chamber membrane were stained with hematoxylin and eosin. The numbers of migrating cells were assessed and counted under a light microscope (Leica DM5000B; Leica Microsystems, Wetzlar, Germany). For each assay, 10 different microscopic fields (×100 magnification) were randomly chosen.

Matrigel Invasion Assay

The Invasion assay was performed using the Boyden chamber system (BD Falcon 8-µm pore, BD353097 with SPL 30024 cell culture plate, 24 well plate, SPL Life Sciences Co. Ltd., Gyeonggi-do, Korea). For the assay BD Matrigel matrix Growth Factor Reduced (BD 356230) was mixed with serum free media in the ratio of 1:15. The transwell inserts were coated with 100 µl mixture in the inner side of transwell and incubated overnight at 37 °C. Prior to seeding the matrirgel matrix mixture was removed from transwell and washed with 100 µl Opti-MEM (Gibco). Following this, siRNA cells were inserted in the upper chamber, approximately 8×10^4 cells in 500 µl of serum free DMEM-F12. The lower chamber was filled with 700 µl medium containing 10% FBS as a chemoattractant. The transwell

chamber was incubated at 37 °C with 5% CO_2 for 24 h. The cells on the upper surface of the filter were then wiped off with a cotton swab and stained with hematoxylin and eosin. The number of cells on lower chamber were counted under a light microscope (Leica DM5000B; Leica Microsystems, Wetzlar, Germany). For each assay, 10 different microscopic fields (×100 magnification) were randomly chosen.

Gelatin Zymography

siRNA treated cells were incubated in DMEM/F-12 containing 0.1% FBS for 72 h. The conditioned medium was collected. To remove the cellular debris the conditioned media was centrifuged at 4500G for 10 minutes at 4 °C. The supernatant media was then concentrated using Amicon Ultra-15 Centrifugal Filter Units (Millipore, Billerica, MA, USA) at 4500G for 80 minutes at 4°C. To analyze MMP-9 activities, 10 µg and 30 µg protein for HN22 and SCC-9 respectively, were loaded onto a gelatin-containing gel (8% acrylamide gel containing 1.5 mg/ml gelatin) and separated by electrophoresis. The gel was renatured in 2.5% Tween-20 solution with gentle agitation for 30 min at room temperature (RT), developed for 72 h at 37 °C in zymogram incubation buffer (50 mM Tris–HCl (pH 7.6) and 5 mM $CaCl_2$), and stained with Coomassie Brilliant Blue R250 (Bio-Rad Laboratories, Hercules, CA, USA). The gel was then de-stained with a solution of 40% methanol and 10% acetic acid until the part of the membrane degraded by MMP-9 became clear. The density of the clear

bands was determined using ImageJ software. Proteins were also run on 8% SDS-PAGE gel as control.

EMT induction using TGF-β

EMT induction was performed using TGF-β (R&D systems, Cat#: 240-B-002 Recombinant human TGF-β1) reconstituted with 4 mM HCl with 0.1% bovine serum albumin to yield a concentration of 10 μg/ml. Cells were seeded in 60 mm dish 10% FBS-PS-containing medium. For treatment with TGF-β cells were serum starved for 24 h by changing the complete media with 0.1% FBS containing medium. Following 24 h, cells were treated using 10 μg/ml TGF-β. For treatment, 1.5 μl of TGF-β was added to 3 ml, to yield 5 ng/ml concentration. Additionally, 3 μl of TGF-β was added to 3 ml, to yield 10 ng/ml concentration. Each plate was washed twice with PBS before medium change and treatment. EMT induction was evaluated following 24 h, 48 h and 72 h. EMT induction experiments were performed using 5 ng/ml concentration of TGF- β for 24 h. PAIP1 interference was performed following TGF- β EMT induction to evaluate the effects of PAIP1 on EMT.

Statistical Analysis

Because of the sparseness in the data set for distant metastasis, the results of the analysis should be regarded as anecdotal. Multivariable correlations between the immunostaining and clinical and histopathological parameters of the tumors were performed via multivariable pearson correlation, student

t-test, chi-square test and fisher's exact test. Additionally, Relative risks were calculated for different variables for high PAIP1 expressions.

Normalized data collected from databases was sorted, tabulated, and stored as excel files and statistically analyzed by applying student *t*-test, one way ANOVA and pearson correlation using SPSS ver. 25.0 and GraphPad Prism 8 and graphically represented using GraphPad Prism 8

The *in vitro* experimental data was statistically analyzed by applying student *t*-test, and one way ANOVA using SPSS ver. 25.0 and GraphPad Prism 8, graphically represented using GraphPad Prism 8 and data was presented as mean ± standard deviation (SD). $p < 0.05$ (two-sided) was considered statistically significant.

III. Results

PAIP1 Amplification across Cancers and in Oral Cancer.

To identify expression of PAIP1 in cancer, *in silico* analysis was performed to evaluate the expression of PAIP1 in different cancer types. Firstly, assessed differentially expressed genes were assessed in 45 normal and 45 cancers from GSE dataset 30784 and found different PAIP1 transcripts to be significantly upregulated (Fig. 1A). Then cBioportal was used to access the TCGA data to analyze the genetic alterations associated with PAIP1. Amplification was the most frequent genetic alteration associated with PAIP1 across various cancers (e.g., Lung squamous, Bladder, Stomach, Uterine, Cervical, Head and neck etc.) (Fig. 1B). A similar pan cancer mRNA analysis was done, and it was seen that PAIP1 mRNA was frequently upregulated in a variety of cancers including Head and Neck Squamous Cell Carcinoma (Fig. 1C). Further copy number vs mRNA expression of HNSC, using the dataset accessed via cBioportal were plotted and it was found that the copy number status positively correlated with mRNA expression (Fig. 2A), pearson linear regression r value 0.81 and *p* value 0.000. The correlation between copy number values and mRNA expression was then assessed in oral cancer cell lines, accessed via CCLE database and a positive correlation was seen between the same (Fig. 2B), pearson linear regression r value 0.707 and *p* value 0.000.

PAIP1 mRNA levels were then analyzed in oral cancer cases via accessing the GEO datasets. PAIP1 mRNA was significantly upregulated in cancer tissues when compared with paired normal adjacent mucosa (GSE dataset GSE37991) (Fig. 3A), paired student *t*-test, *p* value < 0.000. Similarly, PAIP1 mRNA levels were upregulated during the process of carcinogenesis (GSE dataset GSE30784) (Fig. 3B), one way ANOVA, *p* value < 0.0001. A custom cohort was analyzed for oral epithelial tumors from TCGA database and found that the mRNA expression levels of PAIP1 were elevated in cancer tissues when compared to the available values of the normal tissues (Fig. 3C), student *t*-test *p* value 0.0067. PAIP1 mRNA expression was screened (Fig. 3D) in oral cancer cell lines (including HSC2, HSC3, HSC4, HN22, Ca9.22, SCC-9, HO1-N1, HO1-U1; MDA-MB-231) and normal oral keratinocyte cell lines (iHOK). PAIP1 mRNA levels were frequently elevated in different cancer cell lines compared to normal iHOK, significantly upregulated in HN22, HO1-U1, Ca9.22 and SCC-9 compared to other cell lines, one way ANOVA, *p* value < 0.0001.

PAIP1 protein levels, when analyzed from CPTAC database, showed a similar trend, and was significantly upregulated in cancer when compared to normal tissue (Fig. 4A), student *t*-test, *p* value < 0.000. Further immunohistochemical expression was evaluated, in oral cancer case cohort, using semi quantitative scoring in oral cancer tissues and compared the expression levels of PAIP1 between adjacent normal epithelium and oral cancer. PAIP1 levels, based on semiquantitative IHC scores, were

significantly elevated in cancer when compared to normal oral epithelium (Fig. 4B) student *t*-test, *p* value < 0.0001. Protein levels were then screened (Fig. 4C) in cancer cell lines (including HSC2, HSC3, HSC4, HN22, Ca9.22, SCC-9, HO1-N1, HO1-U1; MDA-MB-231) and normal oral keratinocyte cell lines (IHOK). PAIP1 protein levels were frequently elevated in different oral cancer cell lines, significantly upregulated in HN22, HO1-U1, SCC-9 compared to other cell lines, one way ANOVA, *p* value < 0.0001.

Clinicopathological Features Associated with PAIP1 Expression and its Prognostic Implications.

To identify the association between PAIP1 expression and different clinicopathologic variables, multivariable analysis was performed. PAIP1 expression scores were dichotomized as low expression (comprising of negative and low expression cases) and high expression (Fig. 5A). Clinicopathologic variables stratified by PAIP1 expression as low expression and high expression, are listed in Table 3. PAIP1 was found to be significantly correlated with gender, tumor size, LNM and stage (Fig. 5B). Females presented with an increased risk to demonstrate higher expression of PAIP1, relative risk 1.36 (95% CI 1.04,1.76). Incidence of greater tumor size (T3 and T4) were associated with an increased risk of higher PAIP1 expression, relative risk 1.43 (95% CI 1.05,1.96). Additionally, lymph node involvement was found to be associated with high expression of PAIP1 relative risk 1.35 (95% CI 1.07,1.7). With the advanced outcomes of two

variables of TNM stages associated with increased risk in cases of high PAIP1 expression, advanced tumor stages were also associated with higher expression of PAIP1, relative risk 1.52 (95% CI 1.11,2.35) (Fig. 5C). Although, PAIP1 was associated with increased risks of recurrence or with increased age, they were not statistically significant (Fig. 5C).

PAIP1 immunohistochemical expression was significantly elevated in cases of nodal metastasis (Fig. 6A), student *t*-test, *p* value 0.0387. This was found to be in agreement with association of mRNA expression levels with increased incidence of nodal metastasis in GSE78060, student *t*-test, *p* value 0.0238 and TCGA custom cohort (Fig. 6B and C), student *t*-test, *p* value 0.0135.

The immunohistochemical expression levels of PAIP1 increased with worsening TMN stages (Fig. 7A), one-way anova, with multiple comparisons, *p* value 0.0003. Up regulation of PAIP1 levels appeared to correlate with worsening stages of oral cancer in the TCGA cohort (AJCC 7th edition, Stage 4a and Stage 4b combined under Stage 4) (Fig. 7B). Significantly higher values were seen with advanced stages of cancer, one-way anova, with multiple comparisons, *p* value 0.0437. Relation between PAIP1 expression and overall survival of oral cancer patients demonstrated a reduced overall survival of patients with higher expression of PAIP1 (Fig. 7C) meta-analysis of patient overall survival was performed using KM plotter online server (http://kmplot.com/analysis/).

Pattern of Expression of PAIP1 in Different Tumor Regions and Association with Histopathological Features.

To identify the association between PAIP1 expression and different histopathologic variables, multivariable analysis was performed. The staining patterns of PAIP1 was evaluated in different regions of oral cancer classified as Invading front and Main inner mass. Tumor cells in most advanced layer, detached tumor cells and islands at the invading front had higher immunoreactivity for PAIP1 when compared to tumor cells in the inner mass, paired *t*-test, *p* value < 0.0001 (Fig. 8A, B).

Histopathologic variables, stratified by PAIP1 expression, are listed in Table 4. Multivariable analysis was performed, and it was seen that PAIP1 significantly correlated with worse pattern of invasion (Fig. 9A). Increased expression of PAIP1 was associated with a significantly increased risk of non-cohesive patterns of invasion, relative risk 1.38 (95% CI 1.06,1.8) (Fig. 9B). Following this the relation between PAIP1 and different patterns of invasion was analyzed, and it was seen that increased PAIP1 was significantly related with non-cohesive pattern of invasions (Fig. 9 C, D).

Metastatic and Invasive Features associated with PAIP1 siRNA Treated Cells.

To confirm the role of PAIP1 in carcinogenesis and metastatic & invasive potential, PAIP1 was silenced using siRNA interference. Interference

experiment was performed using 25 nM and 50 nM siPAIP1 for 24 and 48 h. PAIP1 was significantly downregulated by both doses at 24 and 48 h (Fig. 10A). Following PAIP1 interference cell viability was evaluated and a significant reduction in SCC-9 cell lines at 50 nM after 24 h and at both doses after 48 h in both cell lines was seen. For evaluation of metastatic features, PAIP1 interference was performed using 25 nM for 24 h (Fig. 10B).

Following, PAIP1 interference, the effects of PAIP1 on colony forming abilities were evaluated and it was found that PAIP1 interference was associated with significant decrease in colony forming abilities in HN22 and SCC-9 cell lines (Fig. 11A), *t*-test, *p* value 0.00. Role of PAIP1 on migratory abilities of oral cancer cells was evaluated and it was seen that downregulation of PAIP1 was significantly associated with decrease in migratory abilities of HN22 and SCC-9 cancer cells on collagen coated transwell assay (Fig. 11B), *t*-test, *p* value 0.00. Inhibiting PAIP1 also significantly reduced the invasive abilities HN22 and SCC-9 cancer cells on matrigel coated transwell assay (Fig. 11C), *t*-test, *p* value 0.00. Interference of PAIP1 was seen to reduce cellular levels of MMP-9 significantly in HN22 but the reduction was not significant in SCC-9, HN22 *t*-test, *p* value 0.01, SCC-9, *p* value 0.373 (Fig. 12A). The effects on the PAIP1 downregulation on the enzymatic activity of MMP-9 were confirmed using gelatin zymography and found a significant decrease in MMP-9 activity in both cell lines (Fig. 12B), HN22 *t*-test, *p* value 0.01, SCC-9, *p* value 0.05.

Effect of PAIP1 on EMT Biomarkers.

To identify the mechanism with which PAIP1 affects invasive and metastatic abilities, EMT markers were evaluated in siPAIP1 treated HN22, no changes were seen in levels of E-Cadherin, N-Cadherin, Vimentin, however there was a slight increase in slug levels (Fig. 13A). Decrease in cellular viability was observed at 48 h and 72 h following TGF-β treatment (Fig. 13B). An increase in N-Cadherin, Vimentin, Snail and Slug was observed following TGF-β treatment (Fig. 13C). PAIP1 interference following TGF-β treatment at 5 ng/ml for 24 h demonstrated a reduction in N Cadherin, Slug, Zeb1 and Vimentin no changes were seen in E Cadherin levels (Fig. 13D).

Effect of PAIP1 on Phosphorylation of c-SRC to Regulate Migration and Invasion.

To identify the mechanism with which PAIP1 affects invasive and metastatic abilities, the intermediate target affecting MMP-9 levels by PAIP1 was examined. A significant reduction in phosphorylated SRC (Tyr416) levels was observed in PAIP1 inhibited HN22 and SCC-9 cell lines (Fig. 14A), HN22 *t*-test, *p* value 0.003, SCC-9, *p* value 0.01. Immunostaining for pSRC (Tyr419) was performed on serial sectioned OSCC cases stained for PAIP1 and found a significant pearson correlation, *p* value 0.0001 and r value 0.55 between PAIP1 expression and pSRC expression (Fig. 14B). The results were in concordance with data accessed via proteomic data commons for

PAIP1 and phosphorylated SRC peptide (LIEDNEyTAR) at the site tyrosine 419, for paired normal and tumor samples (Fig. 15A), pearson correlation, *p* value 0.003 and r value 0.724. Finally, a multivariable analysis was performed to evaluate correlation between PAIP1, pSRC (Tyr419), WPOI and nodal metastasis and found positive correlation between these variables (Fig. 15B). All clinicopathological and histological features with total tumor scores for PAIP1 and pSRC (Tyr419) expression are summarized in Table 5.

IV. Discussion

LNM in oral cancer indicates the poor prognostic outcomes [33]. Here PAIP1 is identified as a prognostic marker, to detect LNM. On analyzing via PANTHERdb (http://geneontology.org/), PAIP1 is associated with biological processes like mRNA stabilization, regulation of translation initiation, positive regulation of translation [34]. In mammalian cells PAIP1 is said to regulate translation initiation by interacting with PABP protein via two motifs [12]. Translational deregulation has been attributed to cellular transformation. It helps the cancer (transformed) cells in adopting to newer phenotypes, conditions, or environments [35]. Eukaryotic initiation factors have been described as a downstream target for mTOR, which may lead to stimulation of Cap dependent translation of oncogenes like MYC, HIF1α etc. during cancer progression. PABP is one of the critical molecules which interacts with EIFs to regulate the translation process. The functions and activity of PABP is regulated by interacting proteins namely, PAIP1 and PAIP2 [5, 7]. It is associated with unfolded protein response (UPR) and has been identified as an upregulated gene in case of ER stress (https://www.gsea-msigdb.org/gsea/index.jsp) [36-38].

UPR is supposed to balance ER folding response under ER stress and in case it fails the cells undergo apoptosis [39]. UPR is driven mainly by IRE1, PERK, and ATF6 [40]. ER stress and UPR can lead to pro apoptotic, anti-apoptotic responses, angiogenic responses, cancer cell dormancy, cell

proliferation [39]. Interestingly, ER stress can also lead to immune resistance and affect metastasis in pancreatic cancer [41] and metastasis in breast cancer [42].

On differential expression analysis PAIP1 was found to be upregulated in oral cancer (Fig. 1A). PAIP1 has been identified as one of the target gene in 5p gain in cervical cancer [9]. The short arm of chromosome 5 is frequently amplified in cancers [10, 43, 44]. This led to a hypothesis that PAIP1 might undergo amplification in head and neck cancer. Concurrent with the hypothesis, most frequent genetic alteration associated with PAIP1 is amplification, and frequent gain in copy number values of PAIP1, followed by mutations, deep deletions, fusions, and multiple alterations in various cancers (Fig. 1B). It was also observed that PAIP1 mRNA levels were frequently upregulated in different cancers (Fig. 1C). The genetic alterations seen in head and neck cancers were mostly amplification with mutations and fusion in few cases. Increased PAIP1 copy numbers were then correlated with PAIP1 mRNA levels and a strong correlation was found between the same (Fig. 2A), suggesting that a gain or amplification in copy number levels of PAIP1 is associated with an increase in PAIP1 mRNA transcripts. Furthermore, the correlation between PAIP1 copy number and mRNA levels was analyzed in the selected cohort from upper aerodigestive cancer cell lines and found a similar pattern (Fig 2B). Suggesting a gain and amplification in PAIP1 copy numbers led to an increase in PAIP1 mRNA levels. To the best of understanding, this is the first time to record this

finding. Differential mRNA expression was identified (Fig. 3D) among oral cancer cell lines and found that the PAIP1 protein expression (Fig. 4C) were upregulated in those cell lines too.

A similar trend of PAIP1 mRNA (Fig 3A-C) and protein levels (Fig 4A and B) overexpression in oral cancers was seen when compared to normal, which is like expression patterns as described in lung, pancreatic, gastric, cervical, and breast tumors [15, 16, 45-48]. PAIP1 was associated with a significant increased risk in greater tumor size, LNM, and advanced stages. PAIP1 expression in oral cancer appears to have a female predilection which has not yet been reported in other tumors (Fig 5B and C) (Table 3). To investigate about the said sexual predilection correlation was evaluated between PAIP1 mRNA levels with AR ESR1, ERBB2, ESR2, PR and protein levels of Her2, and PR (Data not shown), using cBioportal, but there was no significant correlation between any of the factors which were similar to findings in case of breast cancer [46]. Higher PAIP1 expression was also associated with higher risk and positive correlation with greater tumor size, lymph node metastasis (Fig. 6A-C) and advanced stages of the tumor (Fig. 7A and B) and reduced survival (Fig. 7C), consistent with lung, pancreatic, gastric, cervical, breast and hepatocellular tumors [15, 16, 45-48]. Interestingly, Xie et al described similar findings for tongue carcinomas, that PAIP1 was associated with poor prognostic outcomes and positively correlated to tumor size lymph node metastasis and histological grade, however the attached data does not corroborate with the conclusion and

shows an inverse correlation [49].

Tumor cells at the invasive fronts (most advanced layers or detached tumor cells) show molecular heterogeneity when compared to the preceding zones of the tumor, which can better predict the tumor outcomes [31, 50, 51]. An interesting pattern of expression was observed in which the expression levels of PAIP1 were significantly higher in invading zones when compared to inner regions (Fig. 8A). Poor histopathological features like histological differentiation and WPOI were associated with an increased risk with high PAIP expression. PAIP1 was found to positively correlated with advanced WPOI (Fig. 9A and B) (Table 4). Pattern of invasion has been shown to be an important predictor of lymph node metastasis [30, 52]. This is for the first time found that higher PAIP1 was found to be associated with WPOI, significantly greater in non-cohesive patterns of invasions when compared to cohesive patterns of invasion (Fig. 9C and D). Higher incidence of lymph node metastasis, association with worst patterns of invasion, led to the hypothesis that PAIP1 may play a critical role in metastatic cascade.

To confirm the role of PAIP1 in regulating the metastatic process, siRNA silencing of PAIP1 was performed in oral cancer cell lines and found that PAIP1 significantly reduced the colony forming abilities (Fig. 11A), which were consistent with clonogenic abilities lung, pancreatic, gastric, cervical, and breast tumors [15, 16, 46-48].

Inhibition of PAIP1 was also associated with decrease in migratory

abilities of the cells on collagen coated transwell and invasive abilities in Matrigel invasion assay (Fig. 11B and C). The findings are similar to PAIP1 downregulation in lung, pancreatic, gastric cancer cell lines [16, 47, 48].

Effect of PAIP1 inhibition on gelatinase MMPs were investigated. No change in levels of MMP-2 were seen (Data not shown) which contrasted with findings suggested in pancreatic cancer [48]. However, a significant decrease was seen in MMP-9 enzymatic activity (Fig. 12B). This is for the first time it was found that PAIP1 inhibition significantly decreased the cellular MMP-9 level in one cell line (Fig. 12A), but the enzymatic activity of MMP-9 was reduced in both cell lines (Fig. 12B). MMP-9 has been widely described as a mediator of invasion and metastasis. It has been described as potential biomarker for metastasis in cases of oral cancer [53-56].

To analyze the effect on invasive and migratory abilities, the effect of PAIP1 was evaluated on E Cadherin, N Cadherin, Vimentin, Slug, Snail, Zeb1 (Fig. 13A), in contrast to other reports, a significant relationship between PAIP1 and EMT pathway to regulate the metastatic cascade [16, 47, 48] was not seen. However, there was a slight reduction in EMT markers induced by TGF-β (Fig. 13D), but as the phenotypic inhibition was observed independently of EMT induction, led to a hypothesis that a direct kinase target might be affected by PAIP1 to regulate invasive and metastatic features [57, 58].

Activity of MMP-9 is dependent on various factors like fibronectin,

focal adhesion kinase etc [20, 59]. The intermediate signaling kinase molecule was then investigated. c-SRC is a protooncogene which on activation can affect metastatic abilities by affecting MMP-9 activity [60, 61]. It was seen that PAIP1 inhibition did not affect the c-SRC levels, however it significantly reduced the p-SRC (Tyr416/419) (Fig. 14A). This is the first time; it was found that PAIP1 was associated with activation of c-SRC by affecting phosphorylation of tyrosine residue 416/419. However, in contrast to other reports no significant changes were seen in Akt activity (Data not shown) [16]. Paxillin and FAK activity were evaluated, but no significant changes were seen (Data not shown). Following the identification of effect of PAIP1 on phosphorylation of c-SRC, phosphorylated SRC levels were checked in OSCC tissue samples. A similar trend of elevated phosphorylated SRC was seen in the cytoplasm of cancer when compared to adjacent normal mucosa (Data not shown) Expression of phosphorylated SRC were correlated with PAIP1 expression levels in oral cancer and found a positive correlation in oral cancer case cohort and CPTAC HNSCC (Fig. 14B and 15A). Phosphorylation of SRC independently of other kinase molecules, due to PAIP1, may be associated with ER stress and UPR [38]. ER stress has been demonstrated to activate SRC via phosphorylating tyrosine 419 domain [62].

Multi variable analysis was performed for PAIP1 and phosphorylated SRC expression and found that features associated with LNM were positively correlated (Fig. 15B) (Table 5).

The results are indicative of involvement of PAIP1 in LNM and poor prognostic indicators in OSCC, by affecting phosphorylation of c-SRC at tyrosine 419 residue and enzymatic activation of MMP-9. The current goals of the research to establish the association between PAIP1 expression and prognostic indicators of OSCC have been successfully achieved, it does require further validation using larger case cohorts. Although, the current research identifies the intermediate targets affected by PAIP1, it has furnished with prospective research questions on possible effector mechanisms.

V. Conclusion

Current research on association of PAIP1 to different features of oral cancer and the associated mechanism has provided an understanding of the possible processes occurring during LNM associated with PAIP1. Current findings suggest that increased PAIP1 expression increased the possibility of LNM, increase in tumor size additionally it was also positively associated with worse patterns of invasion. The findings corroborated with publicly available data and the PAIP1 silencing experiments *in vitro*, suggesting a utility of PAIP1 as a prognostic marker and a possible application to detect lymph node metastasis prior to treatment, thereby by aiding the surgical plan.

VI. References

1. Sung, H., et al., Global cancer statistics 2020: GLOBOCAN estimates of incidence and mortality worldwide for 36 cancers in 185 countries. CA Cancer J Clin, 2021.
2. Montero, P.H. and S.G. Patel, Cancer of the oral cavity. Surg Oncol Clin N Am, 2015. 24(3): p. 491-508.
3. Pitot, H.C., The molecular biology of carcinogenesis. Cancer, 1993. 72(3 Suppl): p. 962-70.
4. Fares, J., et al., Molecular principles of metastasis: a hallmark of cancer revisited. Signal Transduct Target Ther, 2020. 5(1): p. 28.
5. Sharma, D.K., et al., Role of Eukaryotic Initiation Factors during Cellular Stress and Cancer Progression. J Nucleic Acids, 2016. 2016: p. 8235121.
6. Gallie, D.R., The cap and poly(A) tail function synergistically to regulate mRNA translational efficiency. Genes Dev, 1991. 5(11): p. 2108-16.
7. Kahvejian, A., et al., Mammalian poly(A)-binding protein is a eukaryotic translation initiation factor, which acts via multiple mechanisms. Genes Dev, 2005. 19(1): p. 104-13.
8. Craig, A.W., et al., Interaction of polyadenylate-binding protein with the eIF4G homologue PAIP enhances translation. Nature, 1998. 392(6675): p. 520-3.

9. Scotto, L., et al., Integrative genomics analysis of chromosome 5p gain in cervical cancer reveals target over-expressed genes, including Drosha. Mol Cancer, 2008. 7: p. 58.
10. Tang, W.K., et al., Oncogenic properties of a novel gene JK-1 located in chromosome 5p and its overexpression in human esophageal squamous cell carcinoma. Int J Mol Med, 2007. 19(6): p. 915-23.
11. Martineau, Y., et al., Poly(A)-binding protein-interacting protein 1 binds to eukaryotic translation initiation factor 3 to stimulate translation. Mol Cell Biol, 2008. 28(21): p. 6658-67.
12. Roy, G., et al., Paip1 interacts with poly(A) binding protein through two independent binding motifs. Mol Cell Biol, 2002. 22(11): p. 3769-82.
13. Martineau, Y., et al., Control of Paip1-eukayrotic translation initiation factor 3 interaction by amino acids through S6 kinase. Mol Cell Biol, 2014. 34(6): p. 1046-53.
14. Ivanov, A., et al., Polyadenylate-binding protein-interacting proteins PAIP1 and PAIP2 affect translation termination. J Biol Chem, 2019. 294(21): p. 8630-8639.
15. Li, N., et al., Paip1 Indicated Poor Prognosis in Cervical Cancer and Promoted Cervical Carcinogenesis. Cancer Res Treat, 2019. 51(4): p. 1653-1665.

16. Wang, Y., et al., Paip1 predicts poor prognosis and promotes tumor progression through AKT/GSK-3beta pathway in lung adenocarcinoma. Hum Pathol, 2019. 86: p. 233-242.

17. Irby, R.B. and T.J. Yeatman, Role of Src expression and activation in human cancer. Oncogene, 2000. 19(49): p. 5636-42.

18. Bjorge, J.D., A. Jakymiw, and D.J. Fujita, Selected glimpses into the activation and function of Src kinase. Oncogene, 2000. 19(49): p. 5620-35.

19. Hagedorn, E.J. and D.R. Sherwood, Cell invasion through basement membrane: the anchor cell breaches the barrier. Curr Opin Cell Biol, 2011. 23(5): p. 589-96.

20. Fanjul-Fernandez, M., et al., Matrix metalloproteinases: evolution, gene regulation and functional analysis in mouse models. Biochim Biophys Acta, 2010. 1803(1): p. 3-19.

21. Chen, C., et al., Gene expression profiling identifies genes predictive of oral squamous cell carcinoma. Cancer Epidemiol Biomarkers Prev, 2008. 17(8): p. 2152-62.

22. Barrett, T., et al., NCBI GEO: archive for functional genomics data sets--update. Nucleic Acids Res, 2013. 41(Database issue): p. D991-5.

23. Sheu, J.J., et al., LRIG1 modulates aggressiveness of head and neck cancers by regulating EGFR-MAPK-SPHK1 signaling and extracellular matrix remodeling. Oncogene, 2014. 33(11): p. 1375-84.

24. Cerami, E., et al., The cBio cancer genomics portal: an open platform for exploring multidimensional cancer genomics data. Cancer Discov, 2012. 2(5): p. 401-4.

25. Chandrashekar, D.S., et al., UALCAN: A Portal for Facilitating Tumor Subgroup Gene Expression and Survival Analyses. Neoplasia, 2017. 19(8): p. 649-658.

26. Huang, C., et al., Proteogenomic insights into the biology and treatment of HPV-negative head and neck squamous cell carcinoma. Cancer Cell, 2021. 39(3): p. 361-379 e16.

27. Nagy, Á., G. Munkácsy, and B. Győrffy, Pancancer survival analysis of cancer hallmark genes. bioRxiv, 2020: p. 2020.11.13.381442.

28. Amin, M.B., S.B. Edge, and C. American Joint Committee on, AJCC cancer staging manual. 2017.

29. El-Naggar, A.K., et al., WHO classification of head and neck tumours. 2017.

30. Brandwein-Gensler, M., et al., Oral squamous cell carcinoma: histologic risk assessment, but not margin status, is strongly predictive of local disease-free and overall survival. Am J Surg Pathol, 2005. 29(2): p. 167-78.

31. Carnielli, C.M., et al., Combining discovery and targeted proteomics reveals a prognostic signature in oral cancer. Nat Commun, 2018. 9(1): p. 3598.

32. Livak, K.J. and T.D. Schmittgen, Analysis of relative gene expression data using real-time quantitative PCR and the 2(-Delta Delta C(T)) Method. Methods, 2001. 25(4): p. 402-8.

33. Jin, X., et al., Analysis of clinicopathological characteristics associated with the outcome of oral squamous cell carcinoma and the establishment of tissue microarrays. Oncol Lett, 2016. 12(5): p. 3175-3182.

34. Thomas, P.D., et al., PANTHER: a library of protein families and subfamilies indexed by function. Genome Res, 2003. 13(9): p. 2129-41.

35. Lee, L.J., et al., Cancer Plasticity: The Role of mRNA Translation. Trends Cancer, 2021. 7(2): p. 134-145.

36. Subramanian, A., et al., Gene set enrichment analysis: a knowledge-based approach for interpreting genome-wide expression profiles. Proc Natl Acad Sci U S A, 2005. 102(43): p. 15545-50.

37. Liberzon, A., et al., Molecular signatures database (MSigDB) 3.0. Bioinformatics, 2011. 27(12): p. 1739-40.

38. Coppin, L., et al., Galectin-3 modulates epithelial cell adaptation to stress at the ER-mitochondria interface. Cell Death Dis, 2020. 11(5): p. 360.

39. Yadav, R.K., et al., Endoplasmic reticulum stress and cancer. J Cancer Prev, 2014. 19(2): p. 75-88.

40. Papaioannou, A. and E. Chevet, Driving Cancer Tumorigenesis and

Metastasis Through UPR Signaling. Curr Top Microbiol Immunol, 2018. 414: p. 159-192.

41. Pommier, A., et al., Unresolved endoplasmic reticulum stress engenders immune-resistant, latent pancreatic cancer metastases. Science, 2018. 360(6394).

42. Han, C.C. and F.S. Wan, New Insights into the Role of Endoplasmic Reticulum Stress in Breast Cancer Metastasis. J Breast Cancer, 2018. 21(4): p. 354-362.

43. Vincent-Chong, V.K., et al., Genome wide profiling in oral squamous cell carcinoma identifies a four genetic marker signature of prognostic significance. PLoS One, 2017. 12(4): p. e0174865.

44. Speicher, M.R., et al., Comparative genomic hybridization detects novel deletions and amplifications in head and neck squamous cell carcinomas. Cancer Res, 1995. 55(5): p. 1010-3.

45. Kim, H., et al., High Paip1 Expression as a Potential Prognostic Marker in Hepatocellular Carcinoma. In Vivo, 2020. 34(5): p. 2491-2497.

46. Piao, J., et al., Paip1 affects breast cancer cell growth and represents a novel prognostic biomarker. Hum Pathol, 2018. 73: p. 33-40.

47. Wang, Q., et al., Paip1 overexpression is involved in the progression of gastric cancer and predicts shorter survival of diagnosed patients. Onco Targets Ther, 2019. 12: p. 6565-6576.

48. Guan, H., et al., Role of Paip1 on angiogenesis and invasion in

pancreatic cancer. Exp Cell Res, 2019. 376(2): p. 198-209.

49. Xie, H., et al., Effects of inducing apoptosis and inhibiting proliferation of siRNA on polyadenylate-binding protein-interacting protein 1 in tongue cell carcinoma. Head Neck, 2020.

50. Bryne, M., et al., Malignancy grading of the deep invasive margins of oral squamous cell carcinomas has high prognostic value. J Pathol, 1992. 166(4): p. 375-81.

51. Bryne, M., et al., New malignancy grading is a better prognostic indicator than Broders' grading in oral squamous cell carcinomas. J Oral Pathol Med, 1989. 18(8): p. 432-7.

52. Beggan, C., et al., Pattern of invasion and lymphovascular invasion in squamous cell carcinoma of the floor of the mouth: an interobserver variability study. Histopathology, 2016. 69(6): p. 914-920.

53. Miguel, A.F.P., et al., Association between immunohistochemical expression of matrix metalloproteinases and metastasis in oral squamous cell carcinoma: Systematic review and meta-analysis. Head Neck, 2020. 42(3): p. 569-584.

54. Patel, B.P., et al., Clinical significance of MMP-2 and MMP-9 in patients with oral cancer. Head Neck, 2007. 29(6): p. 564-72.

55. Nanda, D.P., et al., MMP-9 as apotential biomarker for carcinoma of oral cavity: astudy ineastern India. Neoplasma, 2014. 61(6): p. 747-57.

56. Deng, W., et al., Overexpression of MMPs Functions as a Prognostic Biomarker for Oral Cancer Patients: A Systematic Review and Meta-analysis. Oral Health Prev Dent, 2019. 17(6): p. 505-514.

57. Summy, J.M. and G.E. Gallick, Src family kinases in tumor progression and metastasis. Cancer Metastasis Rev, 2003. 22(4): p. 337-58.

58. Patel, A., et al., Novel roles of Src in cancer cell epithelial-to-mesenchymal transition, vascular permeability, microinvasion and metastasis. Life Sci, 2016. 157: p. 52-61.

59. Sen, T., et al., Fibronectin induces matrix metalloproteinase-9 (MMP-9) in human laryngeal carcinoma cells by involving multiple signaling pathways. Biochimie, 2010. 92(10): p. 1422-34.

60. Gautam, J., et al., Down-regulation of cathepsin S and matrix metalloproteinase-9 via Src, a non-receptor tyrosine kinase, suppresses triple-negative breast cancer growth and metastasis. Exp Mol Med, 2018. 50(9): p. 118.

61. Cortes-Reynosa, P., et al., Src kinase regulates metalloproteinase-9 secretion induced by type IV collagen in MCF-7 human breast cancer cells. Matrix Biol, 2008. 27(3): p. 220-31.

62. Tsai, Y.L., et al., Endoplasmic reticulum stress activates SRC, relocating chaperones to the cell surface where GRP78/CD109 blocks TGF-beta signaling. Proc Natl Acad Sci U S A, 2018. 115(18): p. E4245-E4254.

TABLE 1. Clinical Characteristics of OSCC Patients (58 cases)

Variable	No. cases 58 (%)
Age (y); mean, 62.9	
30-39	1 (1.72)
40-49	4 (6.90)
50-59	17 (29.31)
60-69	17 (29.31)
70-79	18 (31.03)
80-89	1 (1.72)
Sex	
Male	34 (58.62)
Female	24 (41.38)
T classification	
T1	11 (18.97)
T2	16 (27.59)
T3	8 (13.79)
T4a	22 (37.93)
T4b	1 (1.72)
N classification	
N0	40 (68.97)
N1	2 (3.45)
N2b	10 (17.24)
N2c	6 (10.34)
M classification	
M0	56 (96.55)
M1	2 (3.45)
Stage	
I	11 (18.97)
II	12 (20.69)
III	3 (5.17)
IV	31 (53.45)
IVb	1 (1.72)
Recurrence	
No	49 (84.48)
Yes	9 (15.52)

TABLE 2. Histological Variables Worst Pattern of Invasion (WPOI) and grade

Variable	No. cases 58 (%)
WPOI	
Type 1	3 (5.17)
Type 2	4 (6.90)
Type 3	26 (44.83)
Type 4	16 (27.59)
Type 5	9 (15.52)
Differentiation status	
Well	52 (89.66)
Moderately	3 (5.17)
Poorly	3 (5.17)

TABLE 3. Association of PAIP1 with clinicopathological features OSCC

Variable	No. of cases (n = 58)	PAIP1		*p*	**Risk Ratio**	**95% CI**
		Negative + Low Expression (n = 13)	High Expression (n=45)			
Age (y)				0.29		
<63	28	8	20		0.86	0.65,1.14
≥63	30	5	25		1.17	0.88,1.55
Sex				**0.02**		
Male	34	11	23		0.74	0.57,0.96
Female	24	2	22		1.36	1.04,1.76
Tumor size				**0.02**		
T1 + T2	27	10	17		0.7	0.51,0.95
T3 + T4	31	3	28		1.43	1.05,1.96
Lymph node metastasis				**0.01**		
Negative	40	12	28		0.74	0.59,0.93
Positive	18	1	17		1.35	1.07,1.7
Distant metastasis				0.53		
Negative	56	12	44		1.57	0.39,6.33
Positive	2	1	1		0.64	0.16,2.56
Stage				**0.01**		
I + II	23	10	13		0.62	0.43,0.9
III + IV	35	3	32		1.52	1.11,2.35
Recurrence				0.26		
No	49	12	37		0.85	0.64,1.12
Yes	9	1	8		1.18	0.89,1.56

TABLE 4. Association of PAIP1 with histopathological features of OSCC

Variable	No. of cases (n = 58)	PAIP1		*p*	**Risk Ratio**	**95% CI**
		Negative + Low expression (n = 13)	High expression (n=45)			
WPOI				**0.02**		
Cohesive (I + II + III)	33	7	22		0.72	0.55,0.95
Non-Cohesive (IV + V)	25	0	23		1.38	1.06,1.8
Differentiation status				0.69		
Well	52	6	40		0.92	0.63,1.36
Moderately to poorly	6	1	5		1.08	0.74,1.6

TABLE 5. Clinicopathological and histopathological features of 58 cases and PAIP1 and pSRC (Tyr419) expression

Case no.	Age	Sex	T 4=4a	N	M	Stage 4=IVA	Recurrence	WPOI	Histological Differentiation	PAIP1	pSRC (Tyr419)
1	49	F	3	2b	n	4	y	4	2	6	5
2	72	F	2	0	n	2	y	3	1	6	6
3	69	M	2	0	n	2	n	3	1	4	5
4	70	M	2	2b	n	4	n	3	1	6	6
5	69	M	1	0	n	1	y	2	1	3	4
6	56	F	4	0	n	4	y	3	1	6	6
7	55	F	2	0	n	2	n	3	1	6	4
8	62	M	2	0	n	2	n	3	1	2	0
9	58	M	1	0	n	1	n	4	1	3	3
10	50	M	2	2c	n	4	n	5	2	6	5
11	71	F	1	0	n	1	n	3	2	5	5
12	53	F	1	0	n	1	n	2	1	3	5
13	63	M	1	0	n	1	n	3	1	0	5
14	52	M	2	0	n	2	n	3	1	5	6
15	66	M	2	0	n	2	n	3	1	5	6
16	79	M	4	2b	n	4	n	3	1	6	5
17	70	F	4	2c	n	4	n	3	1	5	6
18	75	M	2	0	n	2	n	5	1	6	5
19	60	F	2	0	n	2	n	4	1	5	5
20	43	F	2	0	n	2	n	3	1	5	5
21	58	F	4	2b	n	4	n	4	1	6	4
22	51	M	4b	0	y	IVB	n	4	1	3	3
23	74	F	1	0	n	1	n	3	1	5	5
24	67	M	2	0	n	2	n	3	1	4	6
25	61	F	4	2c	n	4	n	4	1	5	6
26	66	M	4	1	n	4	y	3	1	5	5
27	75	F	4	0	n	4	n	3	1	6	6
28	66	M	3	0	n	3	n	4	1	5	6
29	78	M	3	2c	n	4	n	4	1	5	6
30	62	F	4	2b	n	4	n	4	1	6	6
31	77	M	3	0	n	3	n	4	3	6	6
32	71	M	4	0	n	4	n	3	1	5	5
33	68	F	4	0	n	4	y	3	1	5	4
34	81	M	2	0	n	2	n	5	3	5	4

35	74	M	1	0	n	1	n	1	3	0	4
36	56	M	4	0	n	4	n	4	1	6	6
37	47	M	2	0	n	2	n	2	1	0	4
38	58	M	1	0	n	1	n	3	1	0	4
39	55	F	4	0	n	4	n	4	1	5	5
40	39	M	3	2c	n	4	n	5	1	6	5
41	77	F	3	0	n	3	n	4	1	5	5
42	55	M	4	2b	n	4	n	4	1	6	5
43	64	M	1	0	n	1	n	3	1	3	5
44	50	F	1	0	n	1	n	1	1	4	NA
45	42	F	4	0	n	4	y	3	1	5	5
46	70	F	4	0	n	4	n	2	1	5	5
47	74	F	2	2b	y	4	n	5	1	5	3
48	62	M	4	2b	n	4	n	5	1	4	5
49	72	M	4	0	n	4	n	4	1	6	6
50	70	M	4	0	n	4	n	3	1	4	4
51	61	M	4	0	n	4	n	5	1	6	6
52	79	F	3	2c	n	4	y	5	1	6	6
53	50	M	3	2b	n	4	n	3	1	1	5
54	66	F	1	0	n	1	y	1	1	6	NA
55	59	M	2	2b	n	4	n	4	1	5	6
56	56	M	4	0	n	4	n	3	1	6	5
57	63	F	4	1	n	4	n	5	1	6	6
58	52	M	4	0	n	4	n	3	1	5	4

0-2, Negative; <4, Low Expression; >4, High Expression; T, Tumor Size; N, Lymph Node Metastasis; M, Distant Metastasis; WPOI, Worse Pattern of Invasion; n, No; y, Yes; NA, Not Applicable.

Fig 1 PAIP1 amplification across Cancers and Oral cancer. (A) Volcano plot depicting significantly differentially expressed genes, in 45 normal and 45 cancer samples from GSE30784, red upregulated genes, blue downregulated genes, PAIP1 log2 (fold change) 1.217, -log10 (*p* value) 28.329. (B) PAIP1 copy number alterations levels demonstrated frequent amplification across various cancers, using cBioportal. (C) PAIP1 mRNA levels were upregulated across various cancers like Lung, Head and Neck, Esophageal, etc.

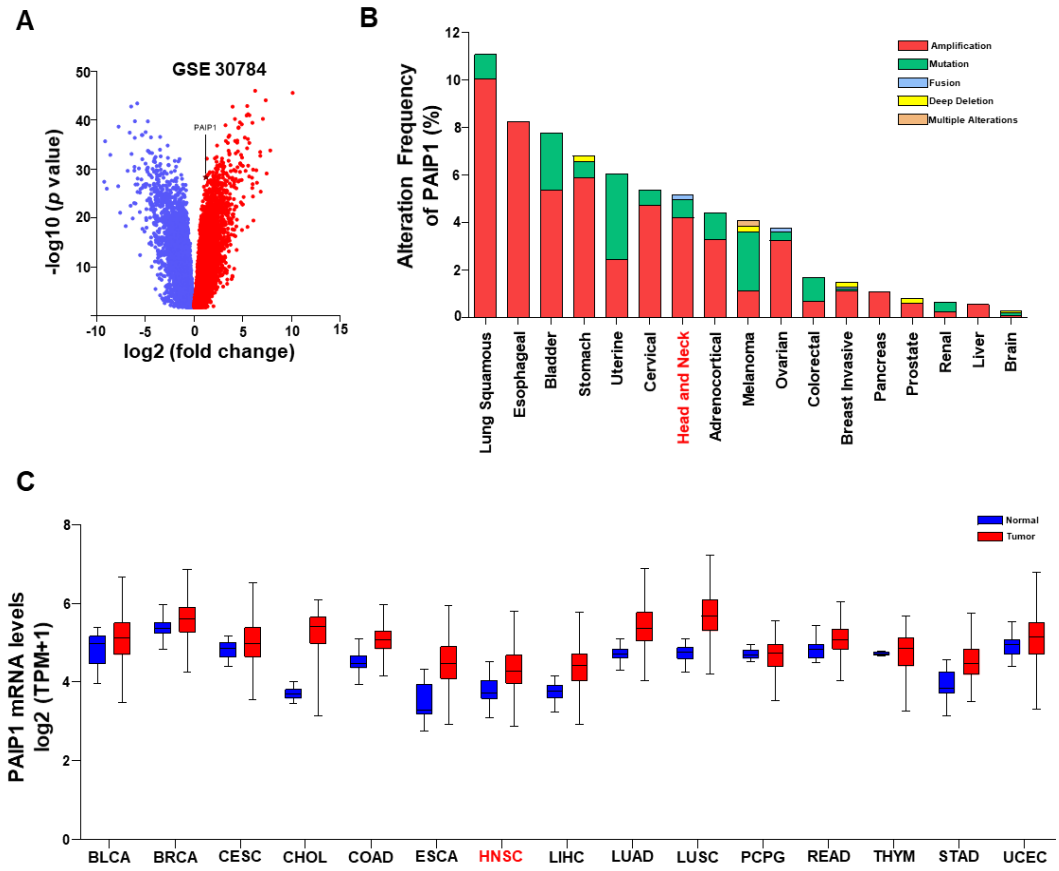

Fig 2 PAIP1 amplification across Cancers and Oral cancer. (A) Positive correlation of PAIP1 mRNA expression levels versus PAIP1 copy number values in head and neck cancers, TCGA data acquired using cBioportal, r value 0.81 *p* value 0.000. (B) Positive correlation of PAIP1 mRNA expression levels versus PAIP1 copy number values in various oral cancer cell lines using CCLE, r value 0.707 *p* value 0.000.

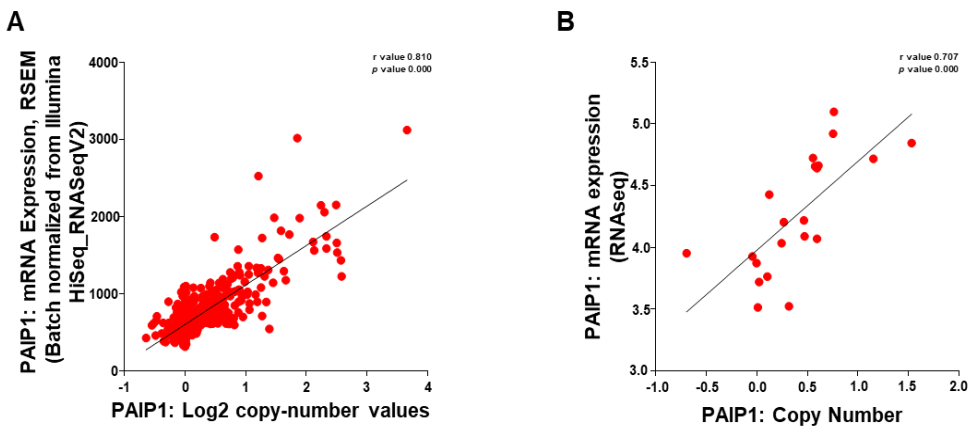

Fig 3 PAIP1 amplification in oral cancer. (A) PAIP1 mRNA levels were significantly upregulated than corresponding adjacent normal epithelium GSE 37991, paired student *t*-test, *p* value < 0.000. (B) PAIP1 mRNA levels were significantly upregulated in cancer when compared to normal and dysplastic epithelium GSE 30784, student *t*-test, *p* value < 0.000. (C) PAIP1 mRNA levels were significantly upregulated in cancer when compared to normal, TCGA custom cohort, student *t*-test *p* value 0.0067. (D) PAIP1 mRNA levels across various oral cancer cell lines and normal oral epithelium cell line & breast cancer cell line, one way ANOVA, *p* value < 0.0001.

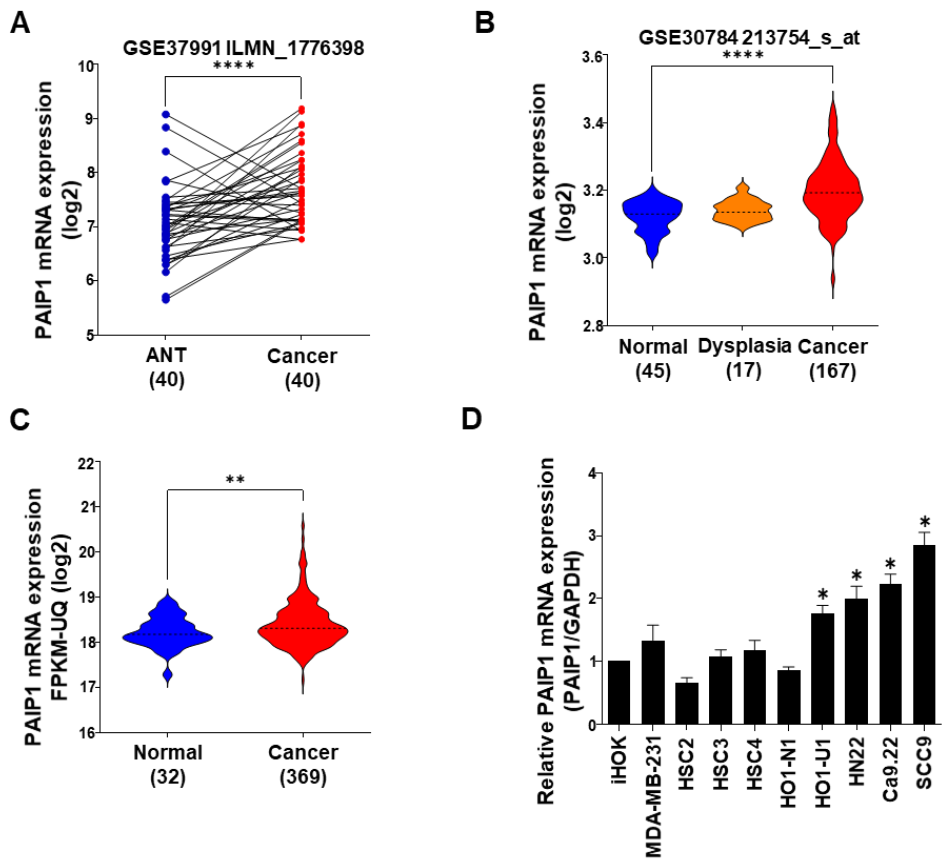

Fig 4 PAIP1 amplification in oral cancer. (A) PAIP1 protein levels were upregulated in cancer when compared to normal tissue, CPTAC, student *t*-test, *p* value < 0.000. (B) Representative image demonstrating areas of normal oral epithelium and oral cancer, no PAIP1 expression in normal oral epithelium and PAIP1 expression in oral cancer, student *t*-test, *p* value < 0.000. (C) PAIP1 protein levels across various oral cancer cell lines and normal oral epithelium cell lines & breast cancer cell line, one way ANOVA, *p* value < 0.0001. Graphs show the mean ± SD of triplicate experiments and significance compared with the vehicle control (* $p < 0.05$).

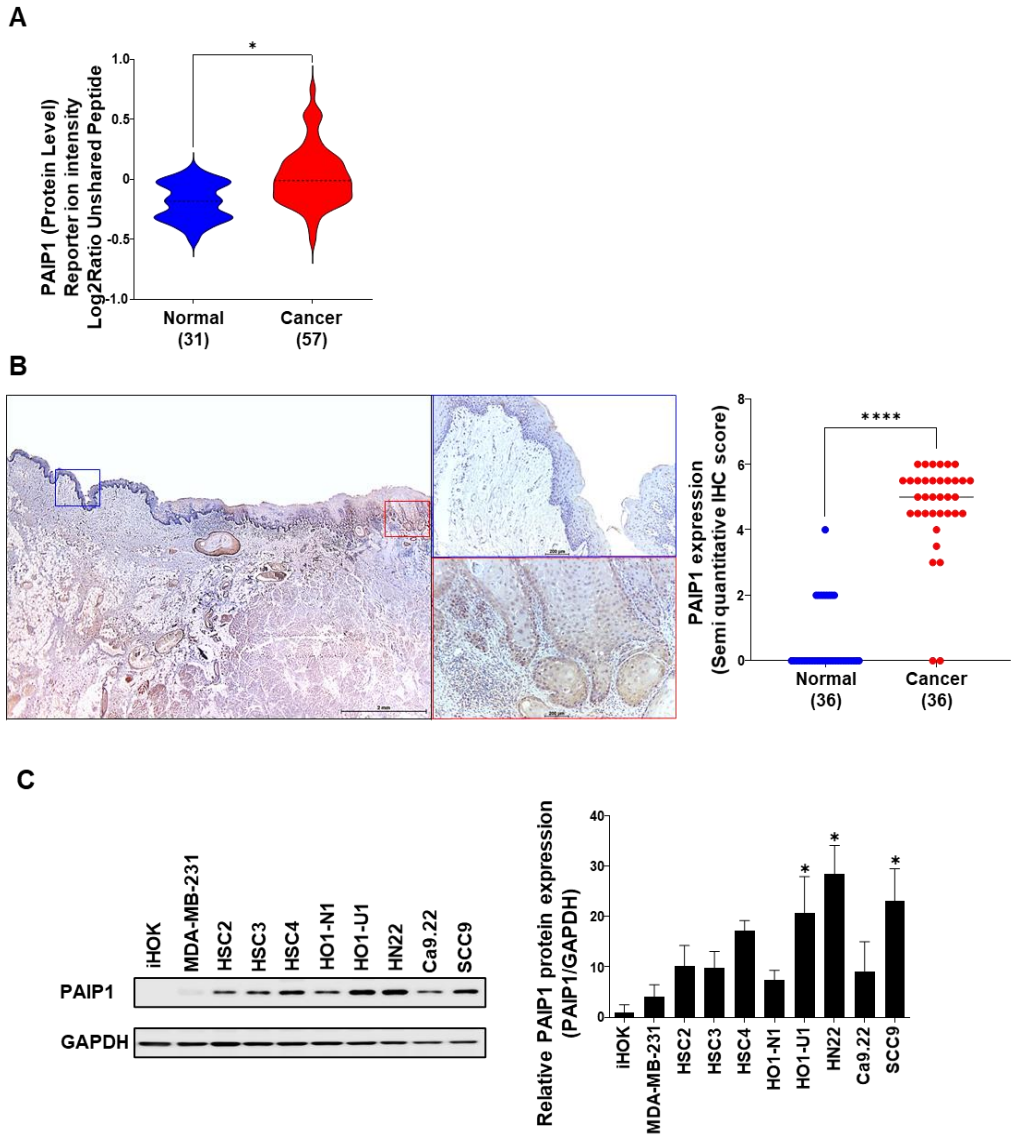
A
PAIP1 (Protein Level)
Reporter ion intensity
Log2Ratio Unshared Peptide
1.0
0.5
0
-0.5
-1.0
*
Normal
(31)
Cancer
(57)
B
PAIP1 expression
(Semi quantitative IHC score)
8
6
4
2
0
****
Normal
(36)
Cancer
(36)
C
iHOK
MDA-MB-231
HSC2
HSC3
HSC4
HO1-N1
HO1-U1
HN22
Ca9.22
SCC9
PAIP1
GAPDH
Relative PAIP1 protein expression
(PAIP1/GAPDH)
40
30
20
10
0
*
*
*
iHOK
MDA-MB-231
HSC2
HSC3
HSC4
HO1-N1
HO1-U1
HN22
Ca9.22
SCC9

Fig 5 Clinicopathologic features associated with PAIP1 expression. (A) PAIP1 expression patterns in OSCC. PAIP1 IHC scores were classified as Negative, Low expression, High expression. (B) Correlation of PAIP1 to different clinicopathological variables. (C) Relative risks associated with high PAIP1 expression.

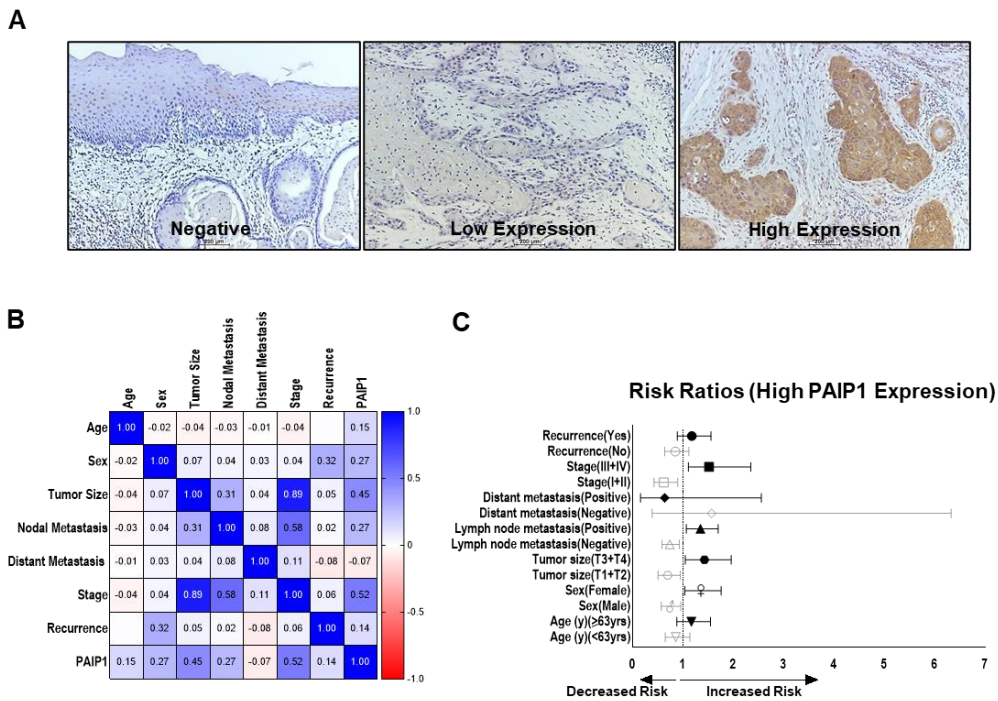

Fig 6 Clinicopathologic features associated with PAIP1 expression. (A) Representative image demonstrating PAIP1 expression in cases with negative and positive nodal metastasis. High PAIP1 expression levels were seen in cases with positive nodal metastasis, student *t*-test, *p* value 0.0387. (B, C) PAIP1 mRNA levels were also upregulated in cases with positive nodal metastasis, (B) GSE 78060, student *t*-test, *p* value 0.0238 (C) TCGA data, student *t*-test, *p* value 0.0135.

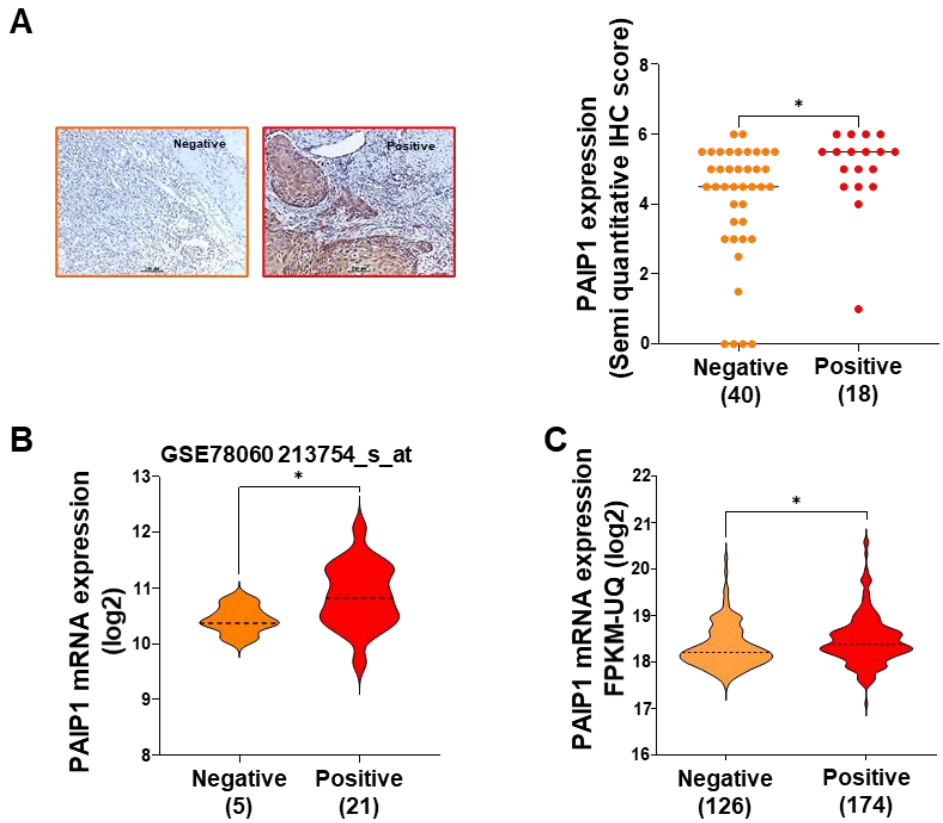

Fig 7 Clinicopathologic features associated with PAIP1 expression. (A) Representative image demonstrating PAIP1 expression levels across different stages of oral cancer. Higher PAIP1 associated with advanced stages of cancer, one way anova, with multiple comparisons, *p* value 0.0003. (B) PAIP1 mRNA levels, from TCGA custom cohort, were significantly upregulated across advanced stages of oral cancer, one-way anova, with multiple comparisons, *p* value 0.0437. (C) Kaplan Meier analysis demonstrates, high PAIP1 expression was associated with decreased overall survival, plot generated using KM plotter [http://kmplot.com/analysis/] for HNSC cohort.

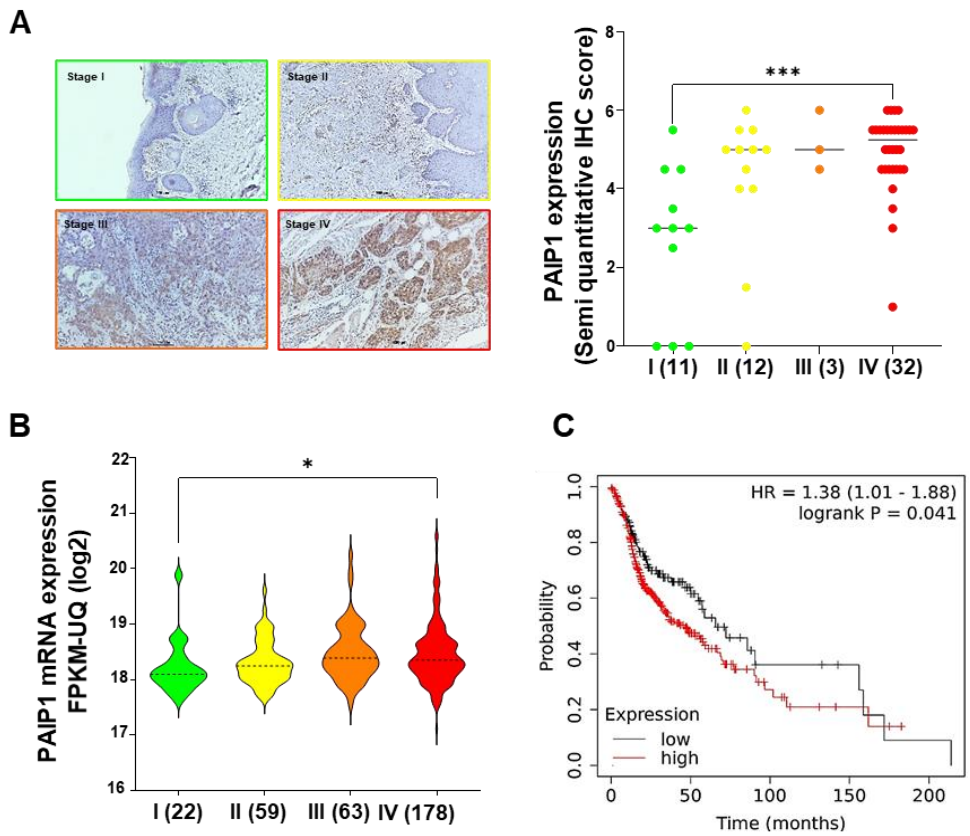

Fig 8 Histopathological features associated with PAIP1 expression. (A, B) (A) Representative image demonstrating lower PAIP1 expression levels in inner portions of the tumor, while higher expression was seen Invading tumor zones, (B) paired *t*-test, *p* value < 0.0001.

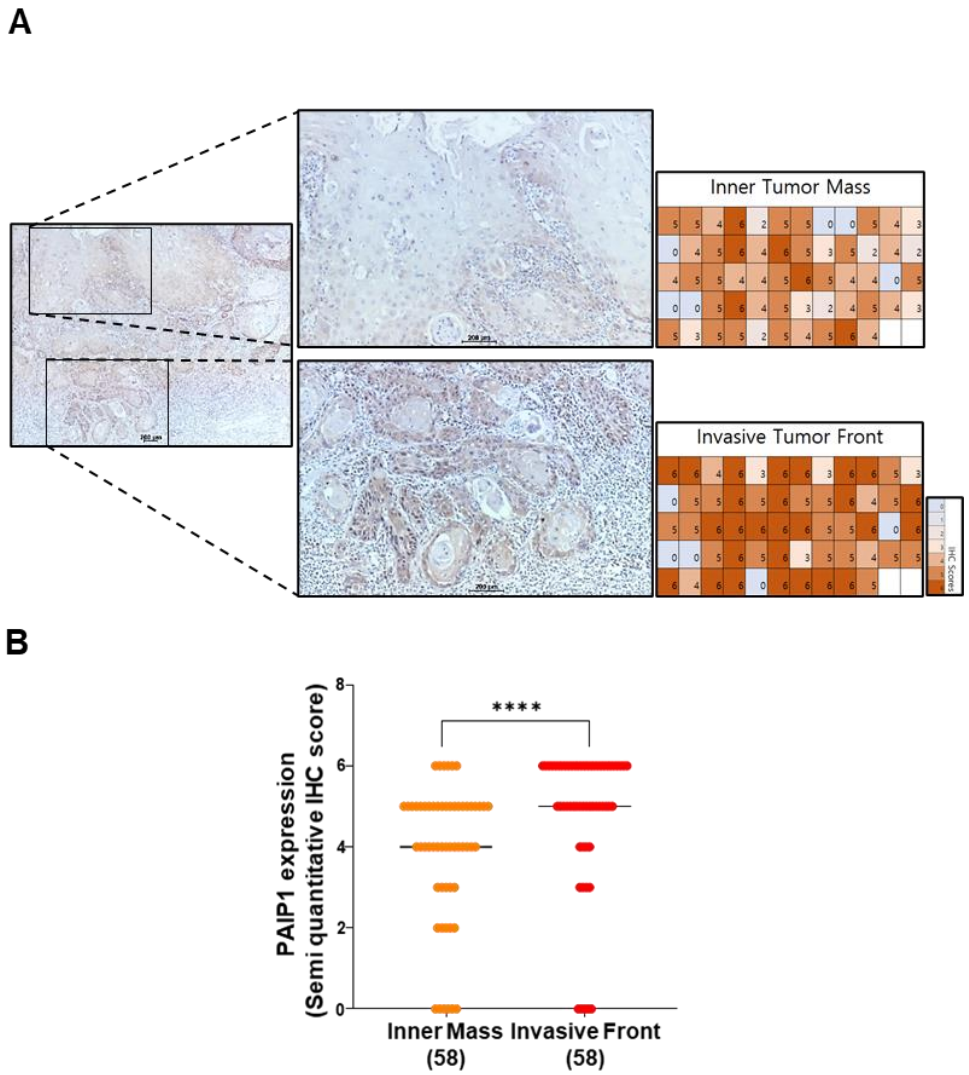

Fig 9 Histopathological features associated with PAIP1 expression. (A) Correlation of PAIP1 to different histopathological variables. (B) Relative risks associated with high PAIP1 expression. (C, D) (C)Representative image demonstrating PAIP1 expression levels in different invasion patterns. Higher expressions were seen in non-cohesive patterns of invasion when compared to cohesive pattern if invasion. Red line depicts 1mm of normal tissue between tumor satellite and tumor interface in Type V. Graphical representation of percentage of cases of varying PAIP1 semiquantitative IHC scores in different types of pattern of invasions and PAIP1, (D) PAIP1 semiquantitative IHC scores in cohesive and non-cohesive POIs, *t*-test, *p* value 0.0031.

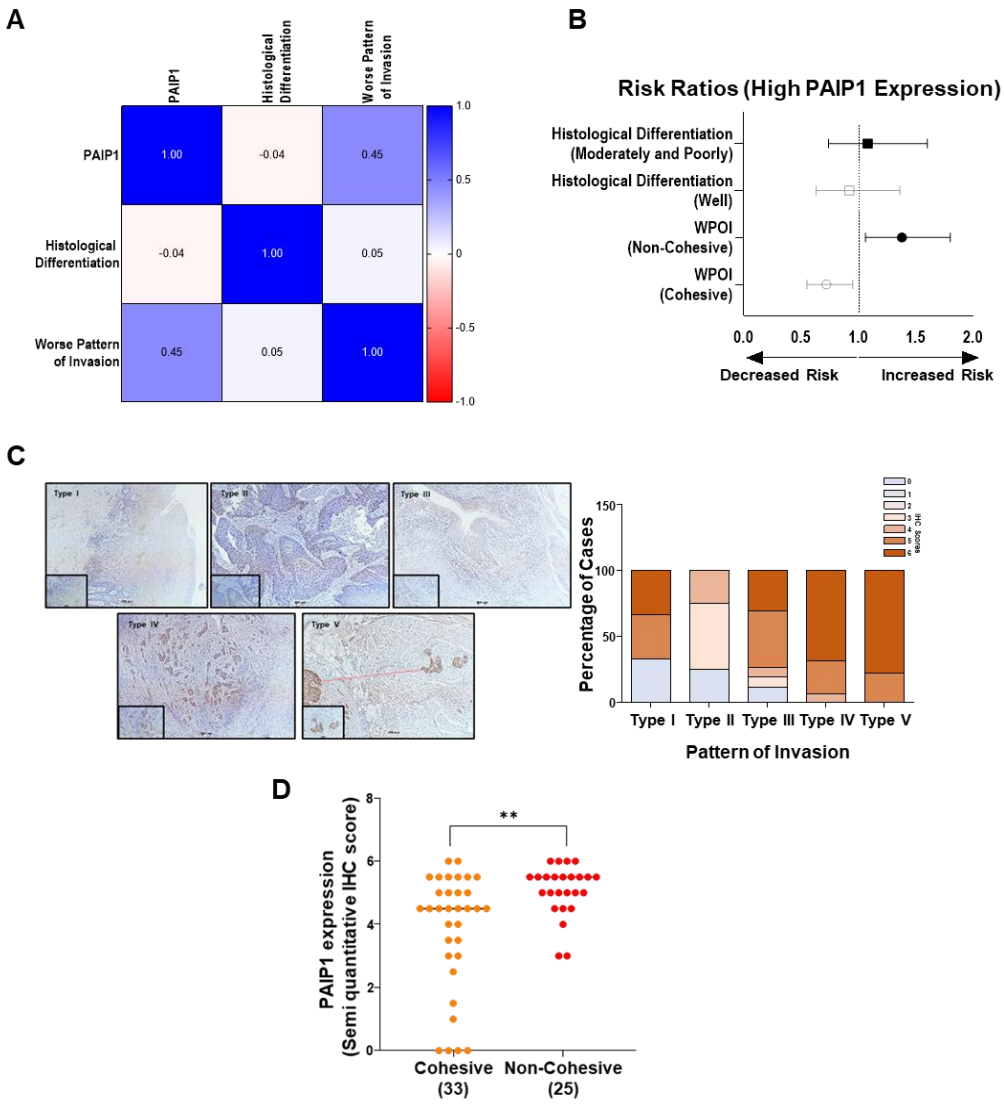
A
PAIP1
Histological Differentiation
Worse Pattern of Invasion
1.00
-0.04
0.45
-0.04
1.00
0.05
0.45
0.05
1.00
1.0
0.5
0
-0.5
-1.0
B
Risk Ratios (High PAIP1 Expression)
Histological Differentiation (Moderately and Poorly)
Histological Differentiation (Well)
WPOI (Non-Cohesive)
WPOI (Cohesive)
0.0
0.5
1.0
1.5
2.0
Decreased Risk
Increased Risk
C
Type I
Type II
Type III
Type IV
Type V
Percentage of Cases
150
100
50
0
IHC Score
Pattern of Invasion
D
PAIP1 expression (Semi quantitative IHC score)
**
8
6
4
2
0
Cohesive (33)
Non-Cohesive (25)

Fig 10 PAIP1 Expression and Interference. (A) Significant reduction of PAIP1 isoform 1 expression following siRNA interference at 25 nM and 50 nM for 24 and 48 h. Protein levels were significantly downregulated, one way anova, *p* value < 0.000. (B) PAIP1 interference decreases the cell viability in HN22 at 25 nM and 50 nM after 48 h, anova, *p* value < 0.000 and in SCC-9 at 50 nM after 24 h and at 25 nM and 50 nM after 48 h, anova, *p* value < 0.000.

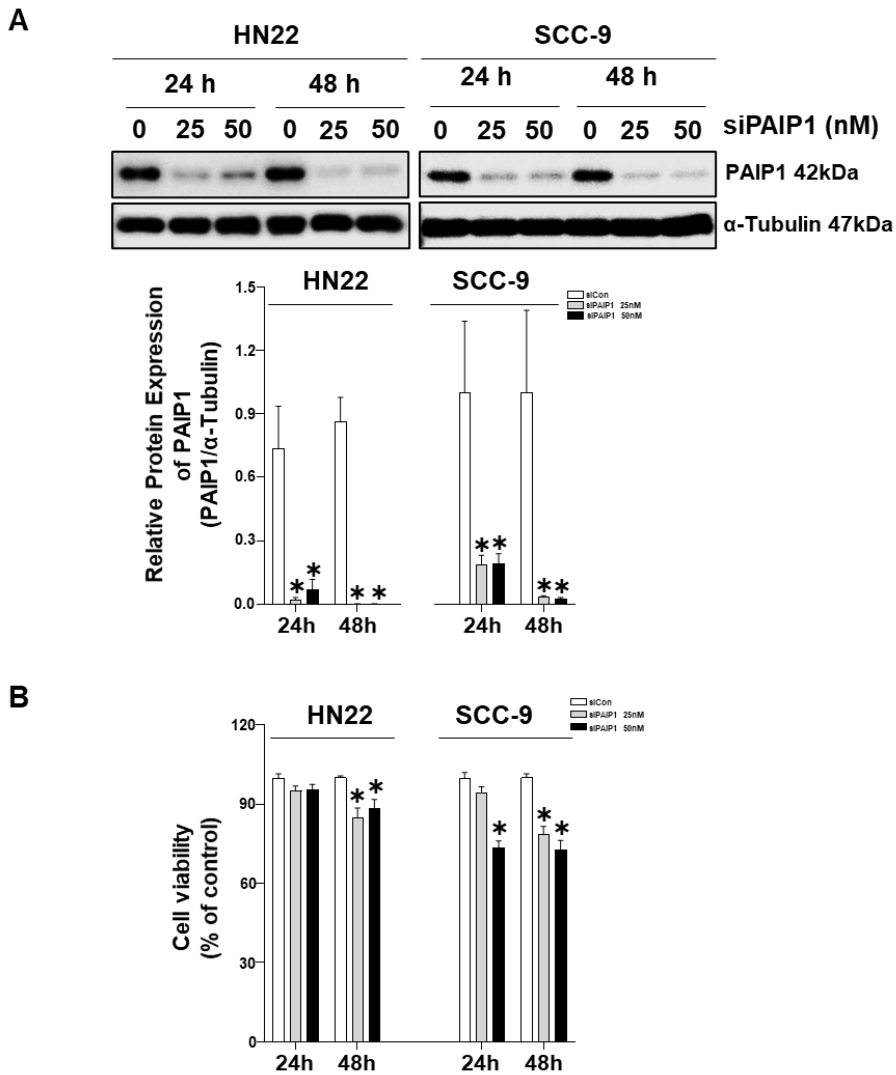

Fig 11 Metastatic and Invasive Features associated with PAIP1 siRNA Treated Cells. (A) PAIP1 inhibition in in HN22 and SCC-9 cells significantly reduced the colony forming abilities, *t*-test, *p* value 0.00. (B) PAIP1 inhibition in in HN22 and SCC-9 cells significantly reduced the migratory abilities on collagen coated transwell assay, *t*-test, *p* value 0.00. (C) PAIP1 inhibition in in HN22 and SCC-9 cells significantly reduced the invasive abilities on matrigel coated transwell assay, *t*-test, *p* value 0.00. (D) PAIP1 downregulation significantly reduced cellular levels of MMP-9 in HN22, but no effect was seen in SCC-9, HN22 *t*-test, *p* value 0.01, SCC-9, *p* value 0.373. (E) PAIP1 inhibition in in HN22 and SCC-9 cells significantly reduced the secreted MMP-9 levels as seen on gelatin zymography, HN22 *t*-test, *p* value 0.01, SCC-9, *p* value 0.05. Graphs show the mean ± SD of triplicate experiments and significance compared with the vehicle control (* $p < 0.05$).

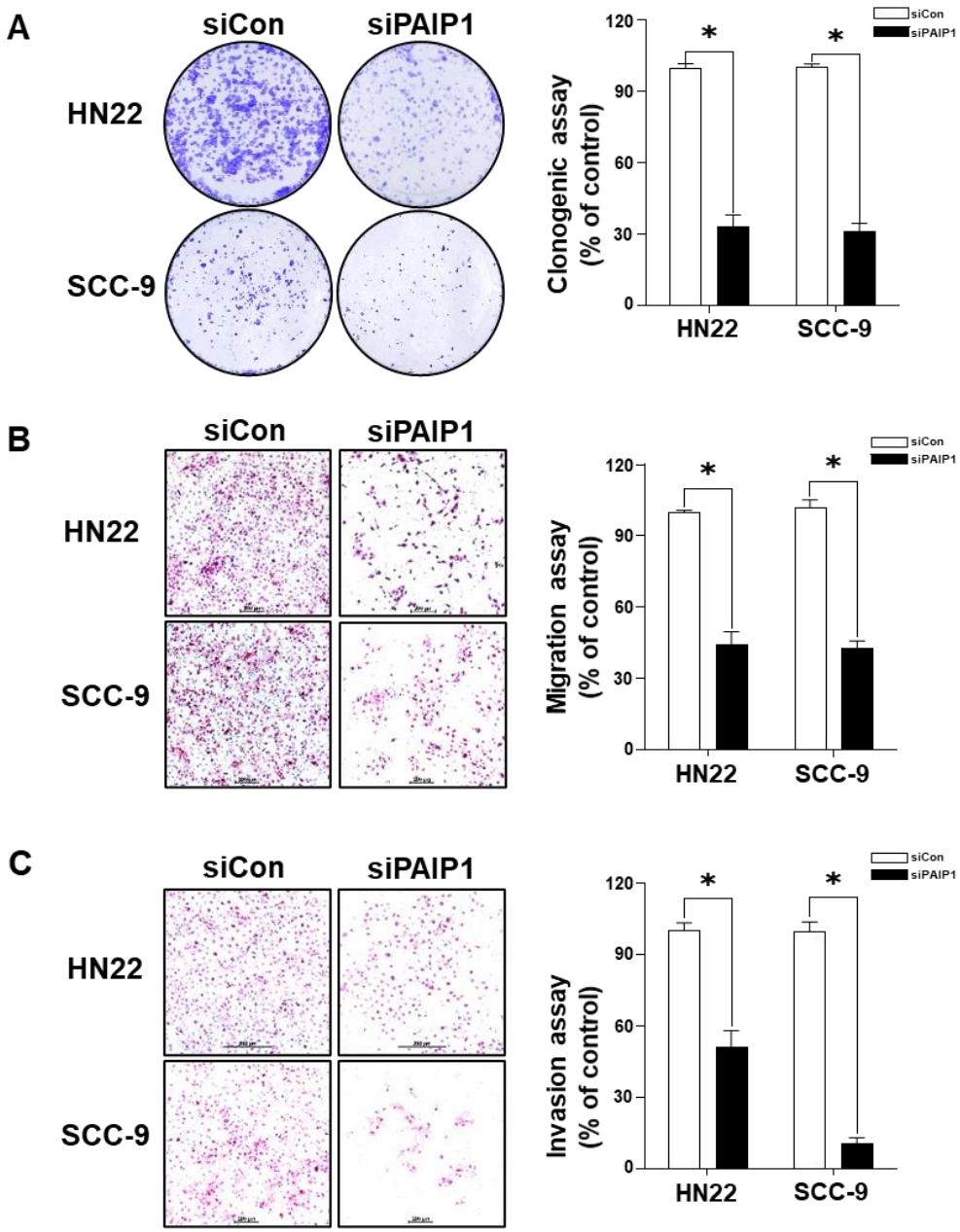
A
siCon
siPAIP1
HN22
SCC-9
Clonogenic assay
(% of control)
siCon
siPAIP1
120
90
60
30
0
*
*
HN22
SCC-9
B
siCon
siPAIP1
HN22
SCC-9
Migration assay
(% of control)
C
siCon
siPAIP1
HN22
SCC-9
Invasion assay
(% of control)

Fig 12 Effect of PAIP1 on MMP-9 cellular levels and enzymatic activity. (A) PAIP1 downregulation significantly reduced cellular levels of MMP-9 in HN22, but no effect was seen in SCC-9, HN22 *t*-test, *p* value 0.01, SCC-9, *p* value 0.373. (B) PAIP1 inhibition in in HN22 and SCC-9 cells significantly reduced the secreted MMP-9 levels as seen on gelatin zymography, HN22 *t*-test, *p* value 0.01, SCC-9, *p* value 0.05. Graphs show the mean ± SD of triplicate experiments and significance compared with the vehicle control (* $p < 0.05$).

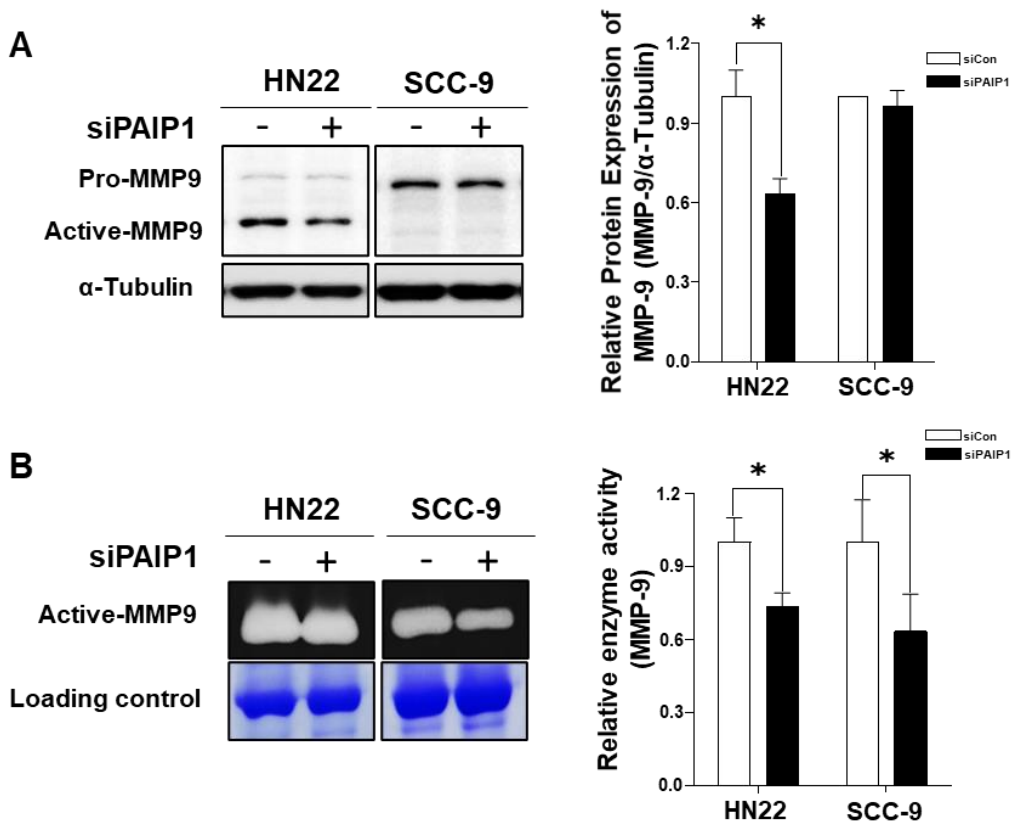

Fig 13 Effect of PAIP1 on EMT markers. (A) PAIP1 downregulation had no effect on E-cadherin, N-Cadherin, Vimentin but an increase in Slug in HN22. (B) EMT induction using TGF-β at 10 ng/ml decreases the cell viability in HN22 after 24, 48 and 72 h and at 5 ng/ml after 48 and 72 h. (C) N-Cadherin, Vimentin, Snail and Slug levels were increased following TGF-β for 24 h. (D) Reduction in N Cadherin, Slug, Zeb1 and Vimentin after PAIP1 interference following TGF-β treatment at 5 ng/ml for 24 h levels.

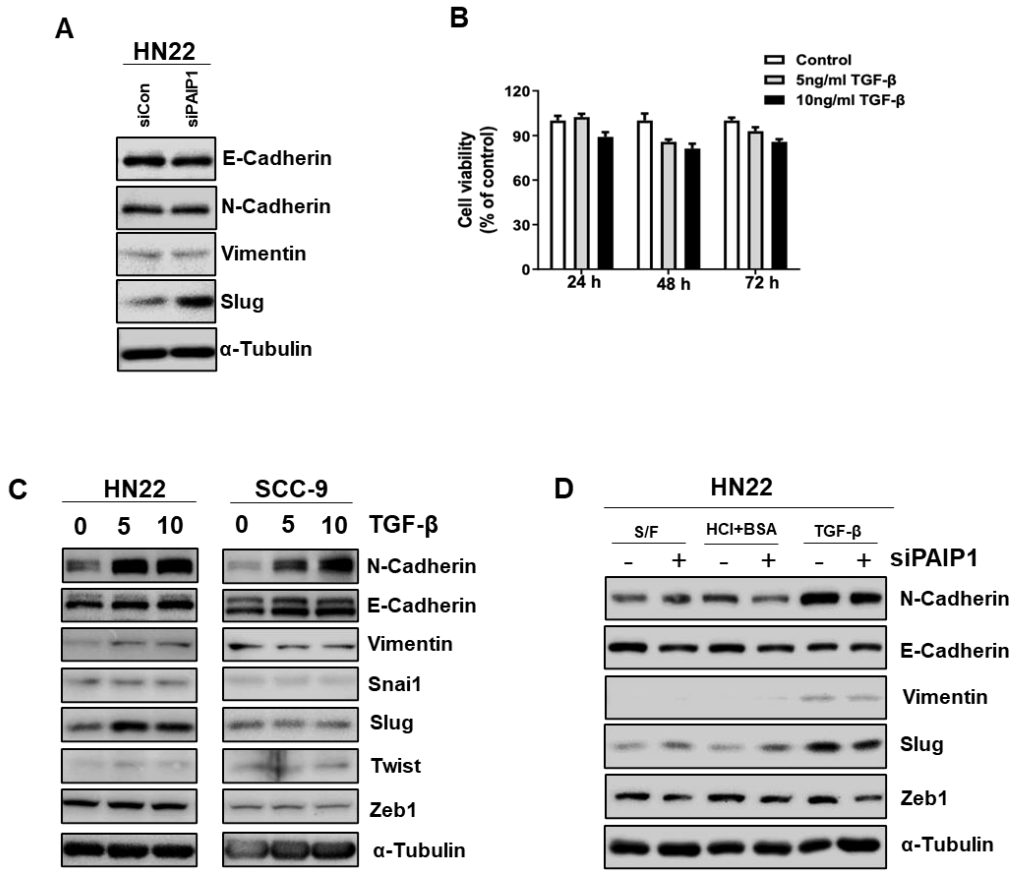

Fig 14 Effect of PAIP1 on phosphorylation of SRC to regulate migration and invasion. (A) PAIP1 inhibition in in HN22 and SCC-9 cells significantly reduced phosphorylation of c-SRC, HN22 *t*-test, *p* value 0.003, SCC-9, *p* value 0.01. Graphs show the mean ± SD of triplicate experiments and significance compared with the vehicle control (* $p < 0.05$). (B) Representative image demonstrating IHC staining of PAIP1 and pSRC (Tyr419) in the same region of the same cases on serial sections for high and low expression groups. The correlation analysis of IHC scores of PAIP1 and pSRC expression levels, pearson correlation, *p* value 0.0001 and r value 0.55.

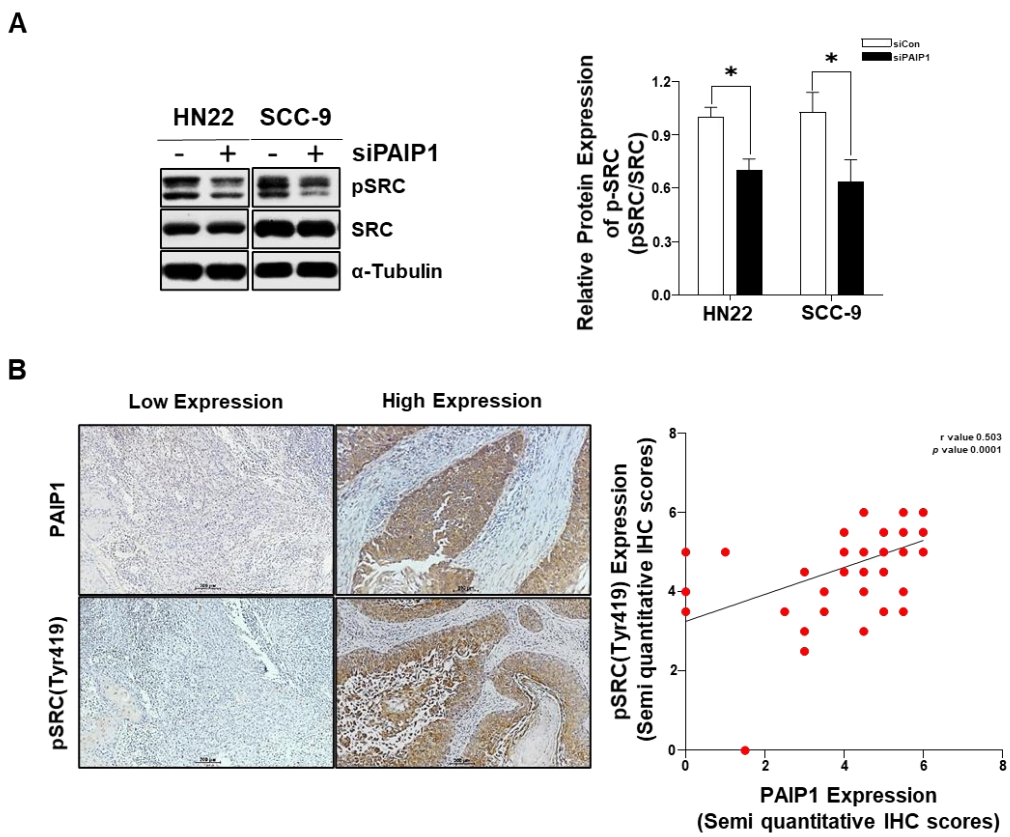

Fig 15 Effect of PAIP1 on phosphorylation of SRC to regulate migration and invasion. (A) Correlation analysis protein levels of PAIP1 and pSRC (LIEDNEyTAR) expression levels in paired normal and tumor HNSCC tissues extracted from CPTAC, pearson correlation, *p* value 0.003 and r value 0.724. (B) Positive multivariable pearson correlation of PAIP1 and pSRC to metastatic and invasive variables.

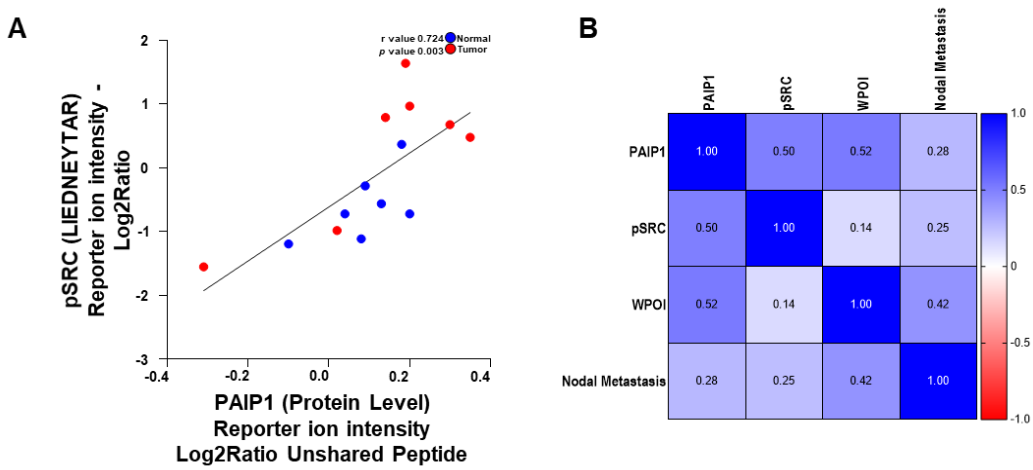

국문초록

PAIP1 발현이 구강 편평 세포 암종에서 전이능과 예후에 미치는영향

구강병리학 전공 **니티** (지도교수 **홍 성 두**)

목적

림프절 전이는 구강 편평 세포 암종의 중요한 예후 지표이며 림프절 전이를 조절하는 바이오 마커는 예후 지표 및 치료 표적으로서 역할을 할 수 있다. 암의 전이과정에서 번역 기계의 조절 장애는 빈번하게 발생하는 것을 특징으로 한다. PAIP1은 번역개시 과정에서 중요한 역할을 하며 다양한 암에서 과발현 되는 것으로 알려져 있으나, 현재까지 구강평편세포암종에서는 전혀 연구된 바 없다. 따라서, 본 연구의 목적은 구강평편세포암종에서 PAIP1의 역할을 규명하고 림프절 전이에 미치는 영향을 밝히고자 한다.

방법

구강편평세포 암에서 PAIP1의 발현을 분석하기 위해 TCGA, CPTAC, GEO 및 CCLE 데이터베이스 등의 공개 도메인에 있는 데이터를 활용한 *in silico* 분석을 실시하였고, 구강편평세포 암종을 지닌 환자조직을 사용하여 PAIP1 발현을 면역조직염색을 통해 다양한 임상병리학적 요인과 비교분석 평가하였다. 또한, PAIP1이 과발현된 구강평편세포암종 세포주에서

siPAIP1을 처리하여 암세포주의 이동과 전이에 PAIP1 미치는 영향을 transwell migration, matrigel invasion assay 및 gelatin zymography를 통해 분석하고 그 메커니즘을 살펴보고자 하였다.

결과

in silico analysis를 통해, PAIP1은 정상 조직과 비교하여 구강암 환자군에서 mRNA 및 단백질 수준이 유의하게 상향 조절됨을 확인하였으며, 림프절 전이를 지닌 환자군에서 PAIP1 mRNA 과발현과의 밀접한 상관관계를 나타내었다. 면역조직염색 결과에서는, PAIP1이 정상 구강 상피와 비교할 때 암에서 유의하게 상향 조절되었으며, 더 강한 발현이 종양 크기 증가, 림프절 전이 및 불량한 침입 패턴과 관련이 있음을 확인하였다. siPAIP1을 처리한 구강암 세포주에서는 집락 형성 능력, 이동성 및 침습성 능력이 현저히 감소하는 것을 발견하였으며, MMP-9 효소 활성이 감소함을 젤라틴 zymography를 이용하여 증명하였다. 이와 더불어, 본 연구는 PAIP1의 과발현이 티로신 잔기 419에서 SRC의 인산화에 영향을 미치는 것을 발견하고 면역조직염색 및 CPTAC 데이터 분석을 통해 구강평편세포암종 환자조직에서 PAIP1의 과발현과 SRC 인산화 사이의 상관 관계를 확인하였다.

결론

본 연구를 통하여, PAIP1의 과발현은 구강평편세포암종의 불량한 예후를

나타내는 림프절 전이와 advanced TNM stage와 밀접한 상관관계가 있음을 확인하였으며, PAIP1의 과발현은 MMP-9의 활성화와 SRC의 인산화에 영향을 미침을 확인하였다. 따라서, 본 연구를 통해 PAIP1의 과발현은 구강평편세포암종의 불량한 예후를 나타내는 진단마커 활용할 수 있음을 제시할 수 있다.

주요어: PAIP-1 단백질, 구강 편평 세포 암종, 침윤, 림프절 전이, 전이.

학 번: 2018-37586